Optimal reliable design of energy-efficient Wireless Body Area Networks

Optimal Reliable Design of Energy-efficient Wireless Body Area Networks

Mohammad Ali Raayatpanah[a,*], Atefeh Abdolah Abyaneh[a], Jocelyne Elias[b] and Angelo Trotta[b]

[a]*Mathematical Sciences and Computer, Kharazmi University; Tehran, Iran.*
[b]*Department of Computer Science and Engineering, University of Bologna, Bologna, Italy*

ARTICLE INFO

Keywords:
Wireless Body Area Network
Network design
Load balancing
Reliability
Energy consumption
Congestion
Relay deployment
Cutting plane algorithm

ABSTRACT

A Wireless Body Area Network (WBAN) is a network of wireless devices that are used to monitor the health of individuals or provide them with information pertinent to their personal health. A WBAN typically consists of multiple sensors and a central sink and it enables the tracking of multiple body signals without the need for cables or other wired connections, allowing for a more comfortable user experience. The used sensors are extremely small and lightweight, making them well-suited for long-term medical monitoring. In this paper, we consider the joint problem of device positioning and data routing in WBANs leveraging relay-based multi-hop communication to address network energy consumption and reliable data transmission, which are two fundamental challenges in the WBAN design. The deployment of a WBAN is the most important factor that impacts both the network lifetime and reliability. On the other side, routing in multi-hop WBANs is of paramount importance for efficient communications between sensors and the centralized hub. For this reason, we define and assign to each relay a concave and non-increasing function (called *reliability function*) which permits to decrease consistently congestion occurrence in the network by balancing relays loads. In this work, we consider the problem of designing an energy-aware routing on WBANs while ensuring that all data are delivered to the sink with a sufficiently large probability. This problem is formulated as a non-convex mixed-integer non-linear programming problem and proven to be NP-hard. We first present an efficient linearization technique for the problem and then propose lower- and upper-bounding schemes for the problem, which can be applied within a cutting plane algorithm-based heuristic to solve the problem. Finally, we evaluate the proposed model with a real topology scenario and compare its performance with the most notable methods presented in the literature. Numerical results show that our model, independently of patient body movement, can transfer data through reliable paths from biosensors to the sink while further offering these options: (1) the probability that each biosensor successfully transfers its data to the sink is adjustable according to the desired application; (2) congestion is limited through a careful balancing of incoming traffic to relays, and (3) a small number of relays is installed, while ensuring an energy-efficient routing of data.

1. Introduction

The rapid development in wireless biomedical devices for the Internet of Medical Things (IoMT) [1, 2] has addressed the public health concern by enhancing the quality of health service at lower cost. In this context, Wireless Body Area Networks (WBAN) are key-enabler tools in healthcare applications and patient monitoring in or out of the hospital [3, 4, 5]. A WBAN consists of several small *biosensors* that are sited below the skin or on the body to collect data about vital signs such as pressure, body temperature, heart rate, and brain condition and then transmit such data through wireless links towards one or more collectors, usually called *sinks*. Figure 1 illustrates a schematic example of WBAN in which multiple medical sensors are deployed on the patient's body. The use of WBANs allows the continuous monitoring of the patient during normal (daily) activities in any place and at any location [6]. By using this technology, biomedical data are shared with healthcare professionals who can detect potential health problems earlier and provide more effective targeted treatment [7]. Hence, developing WBANs has changed the patient monitoring pattern and provided continuous monitoring for them [8, 9]. However, this technology is faced with energy and reliability challenges due to the restricted battery resource-based and power-constraints features of biosensor devices.

*Corresponding author
raayatpanah@khu.ac.ir (M.A. Raayatpanah); Std_Abyaneh@khu.ac.ir (A.A. Abyaneh); jocelyne.elias@unibo.it (J. Elias); angelo.trotta5@unibo.it (A. Trotta)
ORCID(s): 0000-0002-3303-0981 (M.A. Raayatpanah); 0000-0002-0552-2444 (A. Trotta)

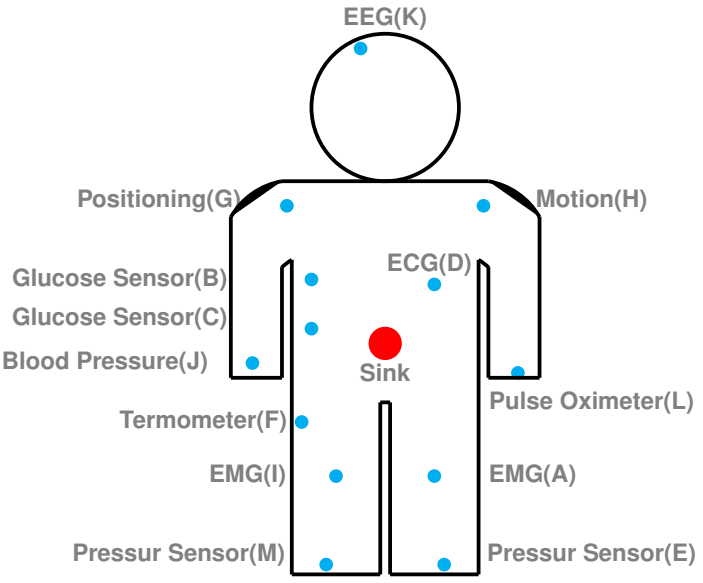

Figure 1: Schematic example of a wireless body area network with different types of biosensors deployed on the human body.

It is important for the WBANs in IoMT that all the sensors are always on to avoid disruption of the patient's data. If a sensor is not functioning properly due to lack of energy resources, it can lead to missed data points that can have an impact on the patient's health and well-being, especially if diagnosis and treatments rely on the data collected by the sensors. Additionally, IoMT relies on a constant stream of data and having a sensor malfunction can disrupt this flow. Keeping all the sensors on at all times ensures that the data is accurate and up-to-date, which helps doctors and medical professionals make the best decisions for their patients [10].

Moreover, the functionality and lifetime of such networks is directly affected by the data transmission over the network, regardless of the wireless technology used (BLE, Wi-Fi, etc.) [11]. Here, reliable transmission is achieved by transferring data through a guaranteed path that avoids losing or delaying data while ensuring an efficient energy consumption, in order not to shorten the WBAN lifetime. Recent literature shows routing data with the purpose of conserving energy can be an appropriate approach to deal with such issues. Generally, two basic methods of transferring data are defined for WBAN, and are called single-hop and multi-hop methods. In the case of direct communication between biosensors and the sink (single-hop), network energy consumption and also signals' interference raise during data transmission operation due to the long distance between network devices [12]. This can decrease network lifetime and also increase delay and path loss. To deal with such problems, a multi-hop communication method has been proposed in the literature [13].

In multi-hop communication, each path from biosensors to its sink contains at least one intermediate biosensor or relay node acting as a data transmitter. Hence, multi-hop communication used in intra-WBANs provides efficient energy consumption due to reducing the distance and path loss between network devices [14].

In our designed network, a multi-hop relay-based communication is employed to route data in which relays and wireless links among them are acting as an intermediate transportation network that does not perform any processing on the data. Our motivation behind using relays as an intermediate node is decreasing the transmission distance between biosensors and relays to improve energy efficiency and network lifetime. Using relays with the purpose of decreasing energy has been proposed in [15], creating a multi-hop based relay routing approach. However, this method led to several challenges, such as the number of relays that would be installed on the body [16], the relay locating problem [17], the relay selecting problem [18, 19], and the way that relays manage data to avoid occurring congestion (or how

to route data through them while preventing the occurrence of node congestion) to have reliable transmission path in each position. The number of relays, which has not been considered in [15], is a major challenge, which can cause issues in patient monitoring. A large number of deployed relays could make patient movement difficult and increase intra-WBAN interference, resulting in packet loss and delayed data delivery. Moreover, released heat due to growing radio frequency signals can hurt sensitive body organs. Therefore, minimizing the number of relays is an inevitable problem in the relay node selection problem. For this latter issue, different criteria can be used, such as remaining sensors' energy, adjacency of the sink [20], noise ratio, and distance [19]. Furthermore, occurring congestion in the network is a common issue regarding a WBAN. Sometimes relays may fail in transferring data due to node congestion as a result of overburdened traffic in selected paths or unbalanced distributions of them [21]. This phenomenon not only leads to delay and packet loss, but also it can highly decrease relay energy resources due to transferring or receiving a huge volume of traffic. Despite the effectiveness of the mentioned methods in reducing the energy consumption of WBAN technology, none have considered the impact of congestion on the reliability and the network lifetime. Here, the reliability is defined as the probability that the data is successfully transmitted from the sensors to the sink through the multi-hop network.

In contrast to the other mentioned routing protocols, we intend to mathematically design and solve the problem of Reliable and Energy-Aware Wireless Body Area Network Design (REAWD) to jointly address the *relay positioning* problem in finding the optimal place for installing a minimum number of relays, as well as the *data routing problem* to find a reliable and energy-efficient path for transferring data to the sink while preventing congestion. In addition, our model is flexible and can be used for a wide range of WBAN applications, since it helps satisfying the following requirements: i) Regardless of the body posture, find a reliable path to transfer data from each biosensor to the sink, and ii) use optimal paths in terms of energy consumption to transfer data. The REAWD problem is formulated as a non-convex mixed-integer non-linear programming (MINLP) problem. Since our model contains bilinear terms in some constraints, in order to find a global optimal solution, we further propose an efficient method for linearizing such terms, which is a non-trivial task using standard linearization techniques because of the continuity of the concerned variables. We perform a thorough evaluation campaign where we evaluate the proposed model and solution techniques in several realistic topology scenarios. We compare their performance with the most notable methods presented in the literature. Numerical results show that our model, independently of patients' body movements, can transfer data through reliable paths from biosensors to the sink while further offering these options: (1) the probability that each biosensor successfully transfers its data to the sink is adjustable by the network administrators; (2) congestion is limited by balancing incoming traffic to relays, and (3) the smallest number of relays is installed, while ensuring an energy-efficient routing of data.

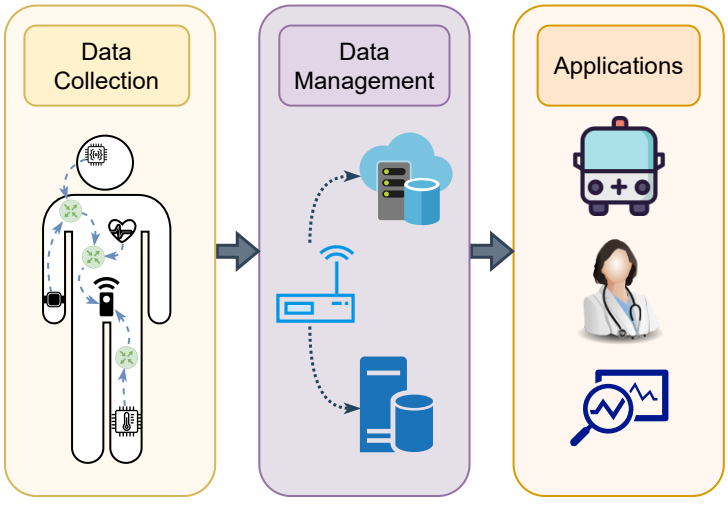

Figure 2: The envisioned IoMT architecture that uses REAWD for data collection.

In Figure 2 is depicted the IoMT architecture that we envision for smart health services. Here, three main modules are designed: (1) *Data Collection* which is in charge of gathering sensory data from the patient; (2) *Data Manage-*

ment which is in charge of collect the data on local and/or cloud data centers; (3) available data will enable several *Applications*, like immediate response in emergency scenarios, smart and remote healthcare via physicists, and data analysis and monitoring. In this work, we focus our research on the *Data Collection* module which enables reliable and energy-aware data gathering. The major contributions of the paper are summarized as follows:

- The introduction of a novel non-convex Mixed Integer Non-Linear Program (MINLP) that minimizes the joint data routing and relay positioning problem under the load on relay nodes and reliability constraints.
- The proof of the NP-hardness of the problem by a reduction from the facility location problem.
- The development of an efficient linearization technique to reformulate the MINLP problem into a mixed-integer linear program and the derivation of upper and lower bounds on the optimal solution value by setting lower- and upper-bounding models for the original MINLP problem.
- The development of a cutting plane algorithm-based heuristic by starting with proper initial solutions and adding valid inequalities.
- The evaluation of the proposed model and heuristic considering different WBAN scenarios and studying the impact of various parameters on the system's performance. Then, the conduction of a comparison between the proposed model and a set of relevant state-of-the-art solutions in terms of energy consumption and data reliability.

The rest of the paper is organized as follows: Section 2 discusses related work. In Section 3, we formulate the REAWD problem as a mathematical program and we address its complexity. We further provide a linearization method that permits to solve it more efficiently in Section 4. Lower- and upper-bounding models, which are presented to derive lower and upper bounds on the optimal solution value, are discussed in Section 5. Section 6 proposes an algorithm for obtaining an optimal solution for the REAWD problem. In Sections 7 and 8, we illustrate the system settings for the WBAN scenario and evaluate the performance of the proposed model and algorithm, respectively. Finally, Section 9 concludes this paper.

2. Related Work

This paper discusses the issues of controlling node congestion, path reliability and network lifetime by looking at both optimal data routing and optimal network device placement problems in WBANs (as a special case of IoT), which are the most struggling issues related to the WBAN quality of service [22, 23, 24]. The majority of energy-efficient methods use single-hop routing communication to provide network reliability for transferring data [25, 26, 27]. An energy-efficient and reliable routing protocol based on single-hop communication is proposed in [25]. The authors worked on a scenario assuming the human body is lying on the bed, while the movement of hands and legs is considered in this work. The proposed protocol, however, does not have any plan to minimize network energy consumption or use it efficiently; hence, all biosensors will likely be short-lived. Reliable data transmission is also not guaranteed due to single-hop communication as well. Chen et al. [26] proposed a cross-layer scheme and MAC-layer protocol implemented on a star topology (single-hop communication) of a WBAN which focuses on energy efficiency and QoS factors such as data rate and delay. Another MAC-layer protocol named Schedule Access MAC protocol has been provided in [27] to deal with the lack of WBAN devices' energy resources. In this article, the simulation is conducted in two scenarios which use single-hop communication. In one scenario, the data rate is kept constant, and the number of nodes changes, while in another it is vice versa.

Although these papers used the single-hop approach as an efficient mechanism for routing data, consuming a large amount of network devices' energy resources through this method can lead to having a network with a shortened lifespan (due to long distances) [28]. The following researches show that using multi-hop communication helps build practical, stronger links, and as a result more reliable networks, and finally, it can be more efficient in minimizing network energy consumption [4, 29]. Multi-hop communication, which is known to reduce transmission range in the network has been divided into two types. The first type uses sensors as intermediate nodes, and the other uses relay nodes [29]. In [30], researchers adopted multi-hop communication paradigms for decreasing network energy consumption. However, the applicability of this method depends on the network topology and might be inefficient in terms of reliability and network lifetime. A combination of single-hop and multi-hop routing mechanisms has been

presented in [22], in which sensors are allowed to transfer data through the multi-hop method if, firstly, they are not a subset of critical sensors, Secondly, their type of sensed data is not critical as well. Otherwise, data would be sent directly using single-hop transmissions. However, using single-hop communication for vital sensors deplete their energy resource in the short term, hence potentially impairing patient monitoring.

In [31], the authors mixed two algorithms (particle swarm optimization and teaching-learning based optimization) in their proposed selecting path problem, in which the objective is to minimize total transition and reception energy consumed by sensors subject to the distance threshold constraints. In this work, multi-hop sensor-based communication is used to transfer data. Also, a sensor is eligible for selection if it has the maximum level of residual energy and minimum distance to the previous sensor deployed in the path. The works that use relays to minimize network energy consumption adopt tailored strategies for routing data such as cooperation [30], relay network [15], Energy-Aware Wireless Body Area Network Design (EAWD) [17], modified EAWD [32] as well as topology design and cross layer optimization [33]. In the *relay network* method, researchers propose a multi-hop communication using relays to ensure Line Of Sight (LOS) communication, so that each biosensor and relay has at least one relay node in LOS [15]. In this work, the number of relays is known and determined through the distance between biosensors and the sink, the path loss coefficient, and the number of sensors [15]. This method can provide energy-efficient and congestion-aware routing; however, all paths are fixed, and if a relay, which lies on a path from one biosensor to the sink, runs out of energy, there is no alternative path to transfer data towards the sink. The authors in [33] propose topology design and cross-layer optimization for WBANs. Specifically, a mathematical programming model is proposed for optimizing single-path routing and relay placement in a WBAN. Their method uses a two-layer tree topology for transferring data from implant biosensors to the sink. For each body region, only one relay is used, and these relays have direct communication with the sink. On the other hand, relays' energy consumption is not considered, while depleting relays' energy resources can cause failures in data delivery. In fact, this work does not consider relay congestion, packet loss, delay and reliability. For comprehensive surveys on relay-based communication, we address the reader to [14, 13, 34].

Few researchers addressed the issue of relay selection, which means that a sensor in the network will act as relay, gathering data from all biosensors in the network and transmitting them to the sink. A relay node selection problem using the Multi-Criteria Decision Making (MCDM) method is presented in [19]. In this article, multiple criteria like traffic load, remaining energy, signal-to-noise ratio, and euclidean distance of biosensors are chosen as a priority in selecting a relay. However, this work considers a wide range of communication for biosensors to transfer data, which has a negative effect on the biosensors' energy resource, raising interference and releasing heat, which can be harmful to body tissues. A meta-heuristic hybrid particle swarm optimization-simulated annealing is suggested in [18] to minimize the network energy consumption of a WBAN. In this work, two different scenarios with four positions are considered. The first scenario only uses the single-hop method to transfer data from biosensors to the sink. The second one uses multi-hop relay-based communication only for the biosensors located at a large distance from the sink. The others transfer their data using single-hop communication. In this research, the authors did not consider how to conserve network connectivity; furthermore, using direct transmission is not a viable approach to optimize WBAN's energy consumption. Hence, none of the two fundamental challenges, energy and reliability, are taken into account. A MAC/routing-based cross-layer protocol is presented in [20] to achieve reliable communication among network devices. Here, reliability is defined as the stability and connectivity of the network. The connectivity is further achieved by biosensors acting as relays. Although this work planned to decrease network energy consumption, only the nodes with the highest amount of energy can act as relay nodes.

Several works show that the placement of relay nodes in a WBAN is an important concern in dealing with energy efficiency, delay and reliability [35, 36, 37]. A cuckoo search algorithm is presented in [16] to locate relays and minimize network energy consumption. In the proposed method, the biosensors near the sink must establish direct communication with this latter. Therefore, due to the weakness of radio frequency signals, the reliability of these routes is not guaranteed. On the other hand, one of the advantages of our proposed REAWD method is to use relay nodes to transfer data from all biosensors to the sink. This permits to compute and prepare alternative paths for biosensors, while preventing at the same time to waste energy due to the decreasing distance between network devices. The importance of locating devices in WBAN and also finding optimal paths to reducing network energy consumption has led to raising the subject of *WBAN design* as a subset of the great category of the Network Design (ND) problem. The decisions must be made in such a way that an effective trade-off between the design decisions' cost and their impact on the whole network functionality is reached. Moreover, the decisions should satisfy the demand and a set of problem constraints [38]. Moreover, ND groups of problems are the subset of the NP-hard class; hence, an algorithm is required to solve these groups of problems efficiently [39].

Author	Year	Algorithm	Advantage	Disadvantage
Sethi et al. [25]	2017	-	Real-data transmission.	Inefficient routing method in terms of energy, considering only one position for the human body.
Chen et al. [26]	2017	-	Reducing delay in packet delivering.	Long distance transmission, inefficient routing method in terms of energy.
Ezhil et al. [27]	2021	-	Using multi-hop communication paradigm, decreasing network energy consumption.	Unable to control node congestion, reliability and network life-span network topology dependently.
Mohammad et al. [22]	2020	-	Using combination of single-hop and multi-hop to reducing energy consumption.	Simplified model, direct communication for transferring critical data, normal data are not allowed to be transferred.
Omodunbi et al. [31]	2022	Teaching-Learning optimization and Particle swarm optimization.	Distance threshold constraints are considered.	Congestion occurrence is not considered.
Ehyaie et al. [15]	2009		Multi-hop relay based communication is used, congestion aware and routing protocol is suggested.	Number of relays is known and determined, paths are fixed, no alternative paths are considered.
Zhou et al. [33]	2017	Multilevel primal and dual. decomposition algorithm	Relay placement problem is considered.	Relays' energy consumption has not been calculated, depleting relays' energy resource can possibly cause failure in data delivering.
Samal et al. [16]	2019	Cuckoo search algorithm.	Relay locating problem and optimizing network energy consumption.	Unreliable transmission, direct transmission for closest biosensors to sink.
Elias et al. [17]	2014	-	Energy efficient routing and cost efficient problem, relay locating problem.	Network reliability and congestion aware routing are not considered.
Bilandi et al. [19]	2021	AHP-Topsis.	Relay node selection problem, using multi-hop sensor-based routing decreasing network energy consumption.	Reliability and congestion are not considered.
Bilandi et .al [18]	2021	Meta heuristic hybrid particle swarm optimization-simulated annealing.	Minimizing network energy consumption, using relay, addressing relay selection problem, evaluating method. with 4 different scenarios.	Relay placement has not been considered Path reliability and node congestion aware routing are not considered.
Abbasi et al. [20]	2021	-	Using relay node in order to provide strong connectivity in the network, define and addressing reliability issue based on stability of network.	Only a node with the maximum amount of remaining energy can act as a relay.
REAWD Model	2022	Cutting plane algorithm-based heuristic.	Design new on-body WBAN by considering body movement, minimizing network energy consumption, considering relay node locating providing reliable and congestion aware path for transferring data, available for other WSN applications.	

Table 1
Summary of the techniques revised in the Related Work section.

All the discussed papers presented methods to deal with energy consumption issues regarding WBANs, but not node congestion-aware routing. Therefore, in this paper, we resent a novel mathematical optimization WBAN design problem to manage both energy-aware and relay node congestion-aware data routing. To handle the complexity of the problem, the idea of executing the exact cutting plane algorithm is expressed [40, 41, 42]. A comprehensive analysis of the techniques reviewed in this section is summarized in Table 1 in terms of their main advantages and disadvantages.

3. Problem Statement

In this section, we provide a formal description of the REAWD problem along with all parameters, optimization variables, motivating example (Section 3.1), and the energy model used to compute the total energy consumed (Section 3.2).

3.1. Network model

In this study, we consider a normal standing scenario with arms hanging along each side, as shown in Figure 1. This topology contains a complete WBAN scenario with different biosensors for various detection purposes. Each biosensor is deployed in a fixed place to sense and gather biomedical data. Biosensors are not eligible to have direct communication with the sink, hence they act as origin nodes. Relay nodes can be attached to the WBAN to gather all

data generated by biosensors and then transmit to the sink via multi-hop routing, in order to increase network lifetime and reliability. The sink device is deployed in the origin of the coordinate system [43].

Hence, the WBAN can be modeled through a digraph $G(V, A)$; the set of vertices V consists of three node types: a set of biosensors B generates data and transmits them to a sink s through a set R of intermediate nodes, called relays (i.e., $V = B \cup R \cup \{s\}$). We assume that the location of all biosensors and the sink has already been determined. Each biosensor $b \in B$ generates a volume of data d^b (expressed in bits/seconds) towards sink s. All data generated by biosensors are transmitted to the sink via multi-hop routing by relays. We indeed assume a QoS-based routing protocol that optimizes the end-to-end transmission path from a biosensor to the sink node, and that the traffic cannot be split over multiple paths. This assumption is a natural choice in WBAN [34].

Relays are a key element of a WBAN, and are needed to collect data from biosensors and transmit it to the sink. The first decision we optimize in our model is the installation of relays; specifically, for each relay $i \in R$, we need to decide whether relay i is deployed or not. Relays are deployed at a unique position over the body. The installation cost of relay i is denoted by c_i, and its capacity (the maximum bitrate that it can manage) is indicated by v_i. The cost c_i may represent the purchasing/monetary cost as well as the maintenance cost of the relay node when this latter is not a one-time device. To manage congestion in relay nodes, each relay node $i \in R$ is associated with a reliability function Re_i, which is a non-increasing function of the amount of data that passes through the relay itself and indicates the probability of successfully transferring data through this relay node. We assume that the reliability functions of relay nodes in the network are mutually independent. Hence, if we consider an end-to-end transmission path P from a biosensor to the sink with intermediate relay nodes r_i, $i = 1, 2, \dots k$, the reliability of path P can be obtained as $\prod_{i=1}^{k} Re_i$. A reliable path is a path that satisfies a given threshold probability parameter. One of the main contributions of this work is selecting a reliable path between each biosensor and the sink. Indeed, data generated by each biosensor $b \in B$ must be successfully transmitted to the sink s with probability at least equal to τ^b, which is a parameter bounded by $0 < \tau^b \leq 1$. We explain the importance of path reliability in a WBAN by the following motivating example.

Motivating Example

Let us consider the WBAN illustrated in Figure 3a, constituted of five biosensor nodes, eight relays and one sink. For simplicity, we assume that all relays have been installed at the same cost. Also, it is assumed that biosensors b_1, b_2, b_3, b_4 and b_5 generate data with rate equal to 4, 2, 3, 2 and 3 (bits/second), respectively.

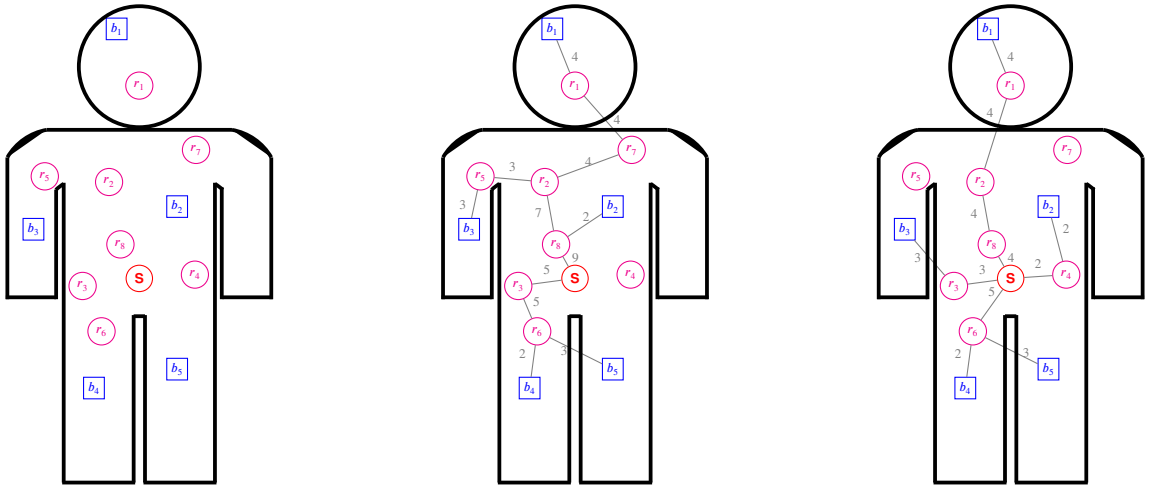

(a) Deployment example. (b) Connections with τ^b=0. (c) Connections with τ^b=0.5.

Figure 3: Problem illustration

To avoid congestion, the reliability of each relay $i \in \{r_1, r_2, r_3, r_4, r_5, r_6, r_7, r_8\}$ is considered as a non-increasing function of the load passing through the relay node itself, i.e., in the form $Re_i = F(l_i)$, $\forall i \in R$. Here, the load l_i is the total sum of data handled by relay i. In most situations, reliability is not affected by a small amount of experienced congestion. On the other hand, when congestion gets heavier, reliability is impaired at an increasing rate. Specifically,

Biosensor	Intermediate relay nodes		Path reliability	
	τ^b=0	τ^b=0.5	τ^b=0	τ^b=0.5
b_1	$r_1 \rightarrow r_7 \rightarrow r_2 \rightarrow r_8$	$r_1 \rightarrow r_2 \rightarrow r_8$	0.07	0.59
b_2	r_8	r_4	0.19	0.96
b_3	$r_5 \rightarrow r_2 \rightarrow r_8$	r_3	0.088	0.91
b_4	$r_6 \rightarrow r_3$	r_6	0.56	0.75
b_5	$r_6 \rightarrow r_3$	r_6	0.56	0.75

Table 2
Results of reliable path selection

following such principle, we consider a reliability function of the form $Re_i = 1 - k(l_i)^2$, k being a constant (which is set guaranteeing that Re only assumes positive values). Since for each relay node i its load is not greater than υ_i (i.e., $l_i \leq \upsilon_i$), then using $k = \frac{1}{\upsilon_i^2}$, $\forall i \in R$, makes sure that $Re \geq 0$. Hence, we consider the following reliability function:

$$Re_i = 1 - (l_i/\upsilon_i)^2, \qquad \forall i \in R. \tag{1}$$

It is clear that for small values of the load passing through each relay, the reliability is very close to 1. However, as relays' load increases, Re tends to decrease steadily, and then sharply. In this example, the capacity $\upsilon_i = 10$ is considered for all $i \in \{r_1, r_2, r_3, r_4, r_5, r_6, r_7, r_8\}$.

To show the importance of reliable paths, we consider two cases for the threshold probability parameter. Let us first assume that there are no reliability constraints, i.e., τ^b=0, $\forall b \in \{b_1, b_2, b_3, b_4, b_5\}$. Multi-hop data routing here is implemented to find the shortest paths based on distance parameters to transmit data from biosensor nodes to the sink and use energy resources efficiently. Concerning this fact, data generated by biosensors in this example would be transferred with the shortest path from biosensor to sink. Intermediate relay nodes in the end-to-end transmission path for each biosensor and the sink node are shown in the second column of Table 2 (with τ^b=0) and in Figure 3b. In the Figures, the numbers shown on the lines define the traffic load over that connection. By calculating the reliability function (1) for relay nodes, we get: $Re_1 = 0.84$, $Re_2 = 0.51$, $Re_3 = 0.75$, $Re_4 = 1$, $Re_5 = 0.91$, $Re_6 = 0.75$, $Re_7 = 0.91$, $Re_8 = 0.19$. Hence, we can obtain the path reliability of each biosensor, which is reported in the third column of Table 2 (with τ^b=0). As we can see, some of these values (like e.g. the reliability for b_1) may in this particular case not be acceptable.

On the other hand, setting a probability threshold parameter would completely change the data routing in this scenario. We assume for example that τ^b=0.5, for all $b \in \{b_1, b_2, b_3, b_4, b_5\}$. In this case, the previous solutions for b_1, b_2, and b_3 are no longer feasible. As we can see in Table 2 and Figure 3c, biosensors have to change their intermediate relay nodes in such new cases. By calculating the reliability function (1) for relay nodes, we get: $Re_1 = 0.84, Re_2 = 0.84, Re_3 = 0.91, Re_4 = 0.96, Re_5 = 1, Re_6 = 0.75, Re_7 = 1, Re_8 = 0.84$. As a main result, the congestion is limited by balancing incoming traffic to relay nods. Hence, relay nodes can live for a long time because their energy consumption is optimized. This motivation example illustrates the importance of reliability functions and the process of routing changes by applying different threshold probability parameters; it also shows that, in practice, we can limit the overall number of installed relays via a careful parameter setting . As we can see in Section 8, for a normal standing scenario with arms hanging along each side with 13 biosensors, the average number of installed relays is four, and we expect that this number is even less for a standing scenario with a lower number of biosensors.

The network performance, in term of overall achievable throughput, in general, improves as the number of relays increases. However, according to [21] and [33], the absorption of radiation will also increase the temperature of body tissues. This can cause damage to sensitive organs by reducing the blood flow and favouring the growth of certain types of bacteria. Due to health considerations and practical deployments on patients, the number of relays to be installed should be reduced. For this reason, we denote U as the maximum number of candidate sites in which relay nodes can be deployed. We also limit the maximum number of relays that can establish a link with sink s by $g \geq 0$. Each relay can establish a wireless link with any other relay, biosensor, and sink located within its communication range. In addition, each biosensor can only be connected to relays within its communication range. Hence, the biosensor coverage parameter, a_{bi}, is defined as a binary parameter which is equal to one if biosensor b establishes a link with relay i. The sink coverage parameter, e_{is}, is defined as well as a binary parameter: when $e_{is} = 1$, it indicates that relay i that has been installed in the WBAN can establish a link with sink s, otherwise it is equal to 0. It should

be noted that a_{bi} depends on the proximity of biosensor b to relay i, as well as on the propagation conditions between such nodes, and e_{is} is related to the distance between relay i and sink s [44].

In the formulation, we present hereafter, it is supposed that there is no direct connection between the biosensor and the sink s. Hence, each path from a biosensor to sink s must pass through at least one relay. The relays support transmissions over shorter distances and thus reduce energy consumption [44]. That means, if a biosensor is so close to the sink, it still sends its data to sink through at least one relay. Since, we aim to minimize the whole biosensors energy consumption. However, our formulation can be easily changed to allow direct communication between biosensors that are close to the sink and the sink itself, if this is the best solution.

Then, link set A is partitioned into two sets of eligible wireless links, based on communication ranges, which are denoted by $\hat{A} \subseteq \{(i,j)|i,j \in R\}$, the set $\hat{A}$ having both incident nodes in R, and $\tilde{A} \subseteq \{(b,j) \cup (j,s)|b \in B, j \in R\}$ which includes all eligible biosensor-relay and relay-sink assignments (i.e., $A = \hat{A} \cup \tilde{A}$). For each relay $i \in R$, we define the forward star, $FS(i) = \{j|(i,j) \in A\}$ and the reverse star, $RS(i) = \{h|(h,i) \in A\}$. Similarly, let $\widetilde{FS}(b) = \left\{i|(b,i) \in \tilde{A}\right\}$ represent the set of relays that can be assigned to biosensors $b \in B$, and also define $\widetilde{RS}(s) = \left\{i|(i,s) \in \tilde{A}\right\}$ as the set of relays that can be assigned to the sink s.

3.2. Energy model

In order to increase the lifetime of the battery nodes, it is necessary to minimize the energy consumed in WBANs. The main sources of energy consumption in WBANs are related to data transmission, data reception, sensing, and processing. In our model, in line with [30, 44, 17], we consider the energy consumption of data transmission and reception, which are the most notable components. Hence, only the communication energy of wireless nodes is considered in this work to calculate the energy consumption in wireless nodes.

To calculate the energy consumption in wireless nodes, let E_{TXelec} and E_{RXelec} denote the energy consumption for transmitting and receiving one unit of data, respectively. The transmission energy of wireless node i to node j over link (i,j) can be computed as

$$E_{trans}(i,j) = p\left[E_{TXelec} + E_{amp}\left(n_{ij}\right) D_{ij}^{n_{ij}}\right]$$

The energy received by wireless node i can be calculated using as

$$E_{rec} = pE_{RXelec}$$

where $E_{amp}(n_{ij})$, D_{ij}, and p are, respectively, the energy for the transmission amplifier, which depends on the path loss coefficient, the distance between nodes i and j, and the total number of transmitted/received bits .

We summarize the notations for all parameters used in this paper in Table 3.

3.3. Mixed-Integer Non-linear programming Formulation

Our non-convex mixed-integer non-linear programming problem tends to locate relays and route data while ensuring the optimal number and placement of installed relays, energy-efficient, and reliable data routing.

We define the decision binary variable x_{bi} to represent the assignment of biosensor b to relay node i:

$$x_{bi} = \begin{cases} 1, & \text{if biosensor } b \in B \text{ is assigned to relay } i \in R, \\ 0, & \text{otherwise.} \end{cases} \tag{2}$$

Similarly, the assignment binary variable x_{is} is introduced to denote the assignment of relay i to sink s:

$$x_{is} = \begin{cases} 1, & \text{if relay } i \in R \text{ is assigned to sink } s, \\ 0, & \text{otherwise.} \end{cases} \tag{3}$$

Decision binary variable y_i is used to represent the installation of a relay node in candidate site i:

$$y_i = \begin{cases} 1, & \text{if a relay is installed in candidate site } i \in R, \\ 0, & \text{otherwise.} \end{cases} \tag{4}$$

We introduce link binary variables z_{ij}^b and f_{is}^b, respectively, that are equal to one if a given link is used by a given traffic as follows:

$$z_{ij}^b = \begin{cases} 1, & \text{if link } (i,j) \in \hat{A} \text{ is used by biosensor } b \in B, \\ 0, & \text{otherwise,} \end{cases} \tag{5}$$

Notation	Meaning
B	Biosensor node set
R	Relay node set
s	Sink node
$\hat{A}$	Set of links between relay nodes
$\tilde{A}$	Set of links between relay nodes, biosensor nodes and sink
$FS(i)$	Forward star of node i
$RS(i)$	Reverse star of node i
E_{RXelec}	Received energy
E_{TXelec}	Transmission energy
E_{amp}	Energy for the transmission amplifier
α	Objective function coefficient
c_i	Cost for installing relay i
U	Maximum number of relays that can be installed (*candidate sites*)
g	Maximum number of relays that can establish a link with sink s
d^b	Traffic generated by sensor b towards sink s
n_{ij}	Path loss coefficient for link (i,j)
D_{ij}	Distance between two nodes i, j
v_i	Maximum capacity of relay i
τ^b	Threshold probability of a successful transmission from biosensor b to sink s
a_{bi}	0-1 connectivity parameter between biosensor b and relay i
e_{is}	0-1 connectivity parameter between relay i and sink s

Table 3
Notations and parameters definition

$$f_{is}^b = \begin{cases} 1, & \text{if link } (i,s) \in \tilde{A} \text{ is used by biosensor } b \in B, \\ 0, & \text{otherwise.} \end{cases} \tag{6}$$

In addition, two continuous variables l_i and Re_i are defined to denote the total amount of traffic passing through relay i and the reliability of relay i, respectively, for all $i \in R$.

In our problem, we need to ensure that each biosensor is assigned only one relay node. We express this constraint as follows:

$$\sum_{i \in \widetilde{FS}(b)} x_{bi} = 1, \qquad \forall b \in B. \tag{7}$$

The eligibility of relays for making connections with biosensors could be fulfilled by satisfying the following constraints.

$$x_{bi} \leq y_i a_{bi}, \qquad \forall b \in B, i \in R. \tag{8}$$

Coherence constraints (8) ensure that a biosensor b can be covered by relay i only if relay i is installed and if b can be connected to j. Similarly, constraints (9) are coherence constraints ensuring that sink s can be covered by relay i only if relay i is installed and if i can be connected to sink s, and constraints (10) impose an upper bound, g , on the number of relays that can be assigned to sink s.

$$x_{is} \leq y_i e_{is}, \qquad \forall i \in R, \tag{9}$$

$$\sum_{i \in \widetilde{RS}(s)} x_{is} \leq g. \tag{10}$$

Data generated by biosensor b are allowed to reach the sink s through relay i as specified by constraint (11).

$$f_{is}^b \leq x_{is} e_{is}, \qquad \forall b \in B, i \in R. \tag{11}$$

The flow balance constraint corresponding to each unit of data transmitted by biosensors $b \in B$ to the sink s at each relay $i \in R$ is stated by constraints (12).

$$\sum_{j \in FS(i)} z_{ij}^b - \sum_{h \in RS(i)} z_{hi}^b = x_{bi} - f_{is}^b, \qquad \forall b \in B, i \in R. \tag{12}$$

The single constraint (13) expresses that the model can deploy at most a number $U > 0$ of relay nodes in the network (U being the number of candidate sites for installing relays).

$$\sum_{i \in R} y_i \leq U. \tag{13}$$

For every relay $i \in R$, constraint (14) defines the relay load as the sum of data collected by all biosensors that transmit to relay i.

$$l_i = \sum_{b \in B} d^b \Big(\sum_{h \in RS(i)} z_{hi}^b + x_{bi} \Big), \qquad \forall i \in R. \tag{14}$$

For each deployed relay $i \in R$, constraints (15) ensure that the relay load is no more than v_i.

$$l_i \leq v_i y_i, \qquad \forall i \in R. \tag{15}$$

To avoid congestion, we define the reliability function of each relay $i \in R$ as a general non-increasing function of the total amount of data passing through it in constraint (16).

$$Re_i = F(l_i) \qquad \forall i \in R. \tag{16}$$

Constraint (17) imposes a reliability threshold inequality for each biosensor to the sink.

$$\left(\sum_{i \in \widetilde{FS}(b)} Re_i x_{bi} \right) \prod_{(i,j) \in \hat{A}} (Re_i)^{z_{ij}^b} \geq \tau^b, \qquad \forall b \in B. \tag{17}$$

In these constraints, for the data generated by each biosensor b transmitting to the sink s, the statement in the parenthesis represents the reliability of the first relay visited in the path by such data. This value is then multiplied by the reliability of all other relays on the path for d^b to calculate the probability of successfully transferring d^b to the sink s.

Our objective is to find the optimal number and placement of relay nodes that minimizes the total cost of deploying relays and the total energy consumption in the network. We formulate them in detail below:

Relay Deployment Cost: The relay deployment cost can be expressed as follows:

$$C_{Deploy} = \sum_{i \in R} c_i y_i. \tag{18}$$

Energy Consumption of Transmitting Traffic: We can compute the total energy consumed by all biosensors to transmit traffic to relay nodes as follows:

$$ET_{trans}^{Bio} = \sum_{b \in B} \sum_{i \in \widetilde{FS}(b)} d^b x_{bi} E_{trans}(b, i). \tag{19}$$

We can calculate the total energy consumed by relays to forward data to other relays and the sink as follows:

$$ET_{trans}^{Relay} = \sum_{b \in B} \left(\sum_{i,j \in R} d^b z_{ij}^b E_{trans}(i, j) + \sum_{i \in \widetilde{RS}(s)} d^b f_{is}^b E_{trans}(i, s) \right). \tag{20}$$

Energy Consumption of Receiving Traffic: The total energy consumed by relays to receive data from all biosensors and other relays.

$$ET_{rec}^{Relay} = \sum_{b \in B} E_{RXelec} \left(\sum_{i \in \widetilde{FS}(b)} d^b x_{bi} + \sum_{i,j \in R} d^b z_{ij}^b \right). \tag{21}$$

Our objective is to minimize both the network deployment cost and the energy consumed by wireless sensors and relays that can be expressed as a weighted sum of the aforementioned costs.

$$\min \left(C_{Deploy} + \alpha(ET_{trans}^{Bio} + ET_{trans}^{Relay} + ET_{rec}^{Relay}) \right) \tag{22}$$

Here, α is a weighting factor that controls the relative importance of the cost components. Note that if we aim at minimizing the maximum energy consumed by relay nodes, we may define the objective function as follows:

$$\min \left(C_{Deploy} + \alpha(max(ET_{trans}^{Relay} + ET_{rec}^{Relay})) \right) \tag{23}$$

In this case, we have a minimax objective which can be transformed by including an additional decision variable T to represent the maximum energy consumption of each relay node in data transmission:

$$T = max(ET_{trans}^{Relay} + ET_{rec}^{Relay})$$

In order to establish this relationship, the following extra constraints must be imposed:

$$T \geq ET_{trans}^{Relay} + ET_{rec}^{Relay}. \tag{24}$$

Now when T is minimized, constraint (24) guarantees that T will be greater than, or equal to, $ET_{trans}^{Relay} + ET_{rec}^{Relay}$. At the same time, the optimal value of T will be no greater than the maximum of $ET_{trans}^{Relay} + ET_{rec}^{Relay}$ because T has been minimized. Therefore the optimal value of T will be both as small as possible and exactly equal to the maximum energy consumption of each relay node in data transmission. Then, the objective function can be written as follows:

$$\min \left(C_{Deploy} + \alpha T \right). \tag{25}$$

3.4. Complexity Analysis

We now reduce the NP-Hard facility Location Problem (FLP) [35] to the REAWD problem. In FLP, we are given a set of potential locations for factories or warehouses with fixed costs, facility costs, and capacities. The objective of the FLP is to select the sites among potential ones so that total cost is minimized. For a simple instance of the REAWD problem, it is assumed that the relays are within the biosensors' communication range, the transmission and reception of data by biosensors and relays are not subject to energy consumption, and we also do not consider reliable path selection and congestion. Suppose that set B is the set of clients who need to be serviced by some potential facility at their location. Let R be the set of facilities. We define a binary variable related to each facility, represented by y_j, which is equal to 1 if facility j is installed for servicing. After that, for each installed facility, a fixed installation cost is considered and expressed by c_j. Meanwhile, we need to assign each client to exactly one facility. To do this, we define a binary variable x_{ij}, which is equal to one if client i is served by facility j. We then consider the cost d_{ij} for serving client i from facility j. The facility location problem seeks to find a $R^* \subseteq R$ such that all clients are covered by facilities while minimizing the total cost of the servicing operation. This problem can be formulated as follows:

$$\min \sum_{j \in R} c_j y_j + \sum_{i \in B} \sum_{j \in R} d_{ij} x_{ij} \tag{26}$$

s.t.

$$\sum_{i \in R} x_{ij} = 1, \qquad \forall i \in B, \tag{27}$$

$$x_{ij} \leq y_j, \qquad \forall i \in B, j \in R \tag{28}$$

$$y_j \in \{0, 1\}, \qquad \forall j \in R, \tag{29}$$

$$x_{ij} \in \{0, 1\}, \qquad \forall i \in B, j \in R. \tag{30}$$

Hereafter we point out the relationship between the two problems:
First of all, the objective function (26) of the facility location problem is similar to the initial part of the REAWD

objective function. Then, constraints (27) and (28) are the same as constraints (7) and (8), since we assume that relays are deployed within biosensors' communication ranges ($a_{ij} = 1\ \forall i \in B, j \in R$). Now, if we can solve this instance of REAWD, we will also get a solution for the FLP. However, FLP is NP-hard, so the REAWD is NP-hard as well. It should be noted that our model contains $O(|R||B|+|A||B|)$ constraints and $O(|R||B|+|R||B||\hat{A}|)$ variables.

4. Linearization of the Mathematical Model

In this section, we develop a linearization technique based on the method presented in [45] to reformulate the non-linear terms in constraints (17). To exchange the non-linear terms in constraints (17) with linear items, firstly, it is needed to define a continuous variable p_i^b that represents the probability of successfully transmitting the data generated by biosensor b to relay i. Therefore, constraints (17) can be replaced by the following inequalities:

$$p_j^b \leq Re_j p_i^b + (1 - z_{ij}^b), \qquad \forall b \in B, (i,j) \in \hat{A}, \tag{31}$$

$$p_i^b \leq 1 - (1 - Re_i)x_{bi}, \qquad \forall b \in B, i \in \widetilde{FS}(b), \tag{32}$$

$$p_i^b \geq \tau^b, \qquad \forall b \in B, i \in R. \tag{33}$$

If arc $(i,j) \in \hat{A}$ lies on the unique path for biosensor $b \in B$, i.e., $z_{ij}^b = 1$, the probability that the data generated by biosensor b successfully reaches relay j is less than or equal to the probability of reaching its preceding node i multiplied by the reliability of arc (i,j). If it is not, i.e., $z_{ij}^b = 0$, then constraint (31) will be a redundant constraint. Similarly, if relay i is the first relay in the unique path for biosensor $b \in B$, i.e., x_{bi}=1, then p_i^b is not larger than Re_i. The reliability threshold is guaranteed by the bound constraint $p_i^b \geq \tau^b$ for each $b \in B$.

The existence of bilinear terms in constraints (31) and (32) makes the problem *non-convex*. Hence, to find a global optimal solution, we need to linearize the non-linear terms, which is a non-trivial task using standard linearization techniques because of the continuity of variables Re_j and p_i^b in the term $Re_j p_i^b$. However, as mentioned earlier, the WBAN consists of a number of biosensors that produce finite amounts of data (bit/s) and each biosensor's data can only be shipped over one path. Hence, the load at each deployed relay can only take a finite number of values. Therefore, the corresponding reliability for each deployed relay can also take only a finite number of values which can be computed using the reliability function given in (16). Using this observation that we have a finite number of possible values for the load and reliability of each deployed relay, we can determine all potential values for l_i, $\forall i \in R$ via the following two-stage method.

- **First stage**

  At first, it is executed a depth-first search starting at relay i, using the links in the reverse direction (i.e., towards the source of data), to determine which biosensors are transferring flow through relay i. Then, using the links in the forward direction (i.e., towards the sink) and executing a depth-first search starting at relay i, again, it is determined whether the sink is reachable from relay i or not. Eventually, let B_i' be the set of biosensors for which their data are transferred towards sink s through relay i.

- **Second stage**

  In this stage, we determine all potential values for the load of relay i, l_i, calculating all possible sums of the form $\sum_{b \in B''} d^b$, for each $B'' \subseteq B_i'$. We can apply dynamic programming to this problem by decomposing it into smaller problems. Without loss of generality we assume that $B_i' = \{b_1, b_2, \ldots, b_{|B_i'|}\}$. Let $w_i(q,k)$ be a binary variable that takes a value of 1 if there exists a subset $B'' \subseteq \{b_1, b_2, \ldots, b_q\}$ such that $\sum_{b \in B''} d^b = k$, for $q = 0, 1, \ldots, |B_i'|$ and $k = 0, \ldots, min\{v_i, \sum_{b \in B} d^b\}$. It should be noticed that $w_i(q,0) = 1$ for all q through the fact that the empty set is a subset of every set. Also, $w_i(q,k) = 0$ for any $k < 0$ because all d^b are positive, and $w_i(0,k) = 0$ for all $k > 0$ since the only subset of the empty set is the empty set which sums to 0. For any $q \geq 1$ and $k > 0$, we have the following recursion: $w_i(q,k) = \max\left\{w_i(q-1,k), w_i(q-1,k-d_s^k)\right\}$.

  Indeed in the recursion $w_i(q,k)$ there are two alternatives depending on whether b_q is considered or not. Consequently, all potential values that l_i can get are associated with those k for which $w_i(|B_i'|,k) = 1$.

We assume that at the end of stage two, set $\Gamma_i = \left\{\gamma_0, ..., \gamma_{G_i}\right\}$ is obtained as all possible values for l_i. Hence, using equation (16), one can derive the corresponding Re_i-values. We denote the set of resulting Re_i using equation (16) by $\Phi_i = \left\{\phi_0, ..., \phi_{G_i}\right\}$. In this case, l_i and Re_i variables can only take distinct values in sets Γ_i and Φ_i, respectively. For this end, we introduce binary variables u_i^g, $\forall i \in R, g \in \left\{0, ..., G_i\right\}$ such that u_i^g=1 if γ_g is chosen for l_i (and also Re_i =ϕ_g), and 0 otherwise. Thus, constraints (14) and (16) can be replaced by the following constraints:

$$\sum_{g=0}^{G_i} \gamma_g u_i^g = \sum_{b \in B} d^b \Big(\sum_{h \in RS(i)} z_{hi}^b + x_{bi} \Big), \qquad \forall i \in R, \tag{34}$$

$$Re_i = \sum_{g=0}^{G_i} \phi_g u_i^g, \qquad \forall i \in R. \tag{35}$$

To make sure that exactly one of the discrete values in sets Γ_i and Φ_i is chosen for variables l_i and Re_i , we consider the following constraints as well:

$$\sum_{g=0}^{G_i} u_i^g = 1, \qquad \forall i \in R, \tag{36}$$

$$u_i^g \in \{0, 1\}, \qquad \forall i \in R. g \in \left\{0, ..., G_i\right\}. \tag{37}$$

After replacing equation (35) in constraints (31) and (32), we get terms either linear or non-linear to form $u_i^g p_i^b$. In the latter case, we have the product of one binary and one bounded continuous variable, which can be replaced by a continuous variable w_{ji}^{gb}=$u_j^g p_i^b$. The following constraints must be added to force w_{ji}^{gb} to take the value of $u_j^g p_i^b$:

$$w_{ji}^{gb} \leq u_j^g, \tag{38}$$

$$w_{ji}^{gb} \leq p_i^b, \tag{39}$$

$$w_{ji}^{gb} \geq p_i^b - (1 - u_j^g). \tag{40}$$

Let χ denote the set of (X, Y, Z, f) that satisfy constraints (2)- (13). Therefore, our MINLP problem using the above linearization modifications can be written as the following equivalent mixed-integer linear program.

$$\min\ C_{Deploy} + \alpha(ET_{trans}^{Bio} + ET_{trans}^{Relay} + ET_{rec}^{Relay})$$

s.t.

$$(X, Y, Z, f) \in \chi \tag{41}$$

$$\sum_{g=0}^{G_i} \gamma_g u_i^g = \sum_{b \in B} d^b \Big(\sum_{h \in RS(i)} z_{hi}^b + x_{bi} \Big), \qquad \forall i \in R, \tag{42}$$

$$\sum_{g=0}^{G_i} \gamma_g u_i^g \leq v_i y_i, \qquad \forall i \in R, \tag{43}$$

$$Re_i = \sum_{g=0}^{G_i} \phi_g u_i^g, \qquad \forall i \in R, \tag{44}$$

$$\sum_{g=0}^{G_i} u_i^g = 1, \qquad \forall i \in R, \tag{45}$$

$$p_j^b \leq \sum_{g=0}^{G_j} \phi_g w_{ji}^{gb} + (1 - z_{ij}^b), \qquad \forall b \in B, \tag{46}$$

$$w_{ji}^{gb} \leq u_j^g, \qquad \forall b \in B, (i, j) \in \hat{A}, g \in \left\{0, ..., G_i\right\}, \tag{47}$$

$$w_{ji}^{gb} \leq p_i^b, \qquad \forall b \in B, (i,j) \in \hat{A}, g \in \left\{0, ..., G_i\right\} \tag{48}$$

$$w_{ji}^{gb} \geq p_i^b + u_j^g - 1, \qquad \forall b \in B, (i,j) \in \hat{A}, g \in \left\{0, ..., G_i\right\} \tag{49}$$

$$p_i^b \leq 1 - (x_{bi} - \sum_{g=0}^{G_i} \phi_g o_{bi}^g), \qquad \forall b \in B, i \in \widetilde{FS}(b), \tag{50}$$

$$o_{bi}^g \leq u_i^g, \qquad \forall b \in B, i \in \widetilde{FS}(b), g \in \left\{0, ..., G_i\right\} \tag{51}$$

$$o_{bi}^g \leq x_{bi}, \qquad \forall b \in B, i \in \widetilde{FS}(b), g \in \left\{0, ..., G_i\right\} \tag{52}$$

$$o_{bi}^g \geq x_{bi} + u_i^g - 1, \qquad \forall b \in B, i \in \widetilde{FS}(b), g \in \left\{0, ..., G_i\right\} \tag{53}$$

$$p_i^b \geq \tau^b, \qquad \forall b \in B, i \in R, \tag{54}$$

$$u_i^g \in \{0,1\}, \qquad \forall g \in \left\{0, ..., G_i\right\}, i \in R, \tag{55}$$

$$o_{bi}^g \in \{0,1\}, \qquad \forall g \in \left\{0, ..., G_i\right\}, i \in R, b \in B, \tag{56}$$

$$w_{ji}^{gb} \geq 0, \qquad \forall b \in B, (i,j) \in \hat{A}, g \in \left\{0, ..., G_i\right\}, \tag{57}$$

$$p_i^b \geq 0, \qquad \forall i \in R, b \in B. \tag{58}$$

As we can see, the size of the MILP problem depends on value of G_i. Hence, the proposed MILP problem cannot provide solutions for large values of G_i within practical computational limits. In the next section, we propose an alternative solution methodology to handle instances of larger sizes.

5. Lower- and Upper-Bounding Scheme

Since the REAWD problem is NP-hard and the MILP proposed in the previous section cannot provide solutions in large size network instances, we propose hereafter lower and upper-bounding models to solve the REAWD problem in a reasonable time. In the following, we describe the lower bounding model, and then the upper bounding model can be formulated in the same manner. One of the main issues for the MINLP problem is related to constraints (16) and (17). Hence, we present the lower bounding model by reformulating these constraints. We first replace constraints (17) with equivalent constraints (31), (32), and (33). Then, we substitute the estimated values of l_i and Re_i as explained below into the constraints.

To estimate values for l_i and Re_i, we select $\beta + 1$ possible values for l_i, similarly to the approach explained in Section 4, and represent them in sorted set $\left\{\gamma_0, \dots, \gamma_\beta\right\}$, where $\gamma_j < \gamma_{j+1}$ for each $j = 0, \dots, \beta - 1$. Since each relay node appears exactly once in each path, the smallest and largest possible values of l_i are 0 and $\sum_{b \in B} d^b$, respectively. Then, we can set $\gamma_0 = 0$ and $\gamma_\beta = \sum_{b \in B} d^b$ to ensure that the actual load of relay i stays within interval $\left[\gamma_0, \gamma_\beta\right]$. The value of Re_i can be computed using the reliability function (16) using γ_j for each $j = 0, \dots, \beta$ and form the set $\left\{\phi_0, \dots, \phi_\beta\right\}$. It is clear that $\phi_0 = 1$ and $\phi_g \geq \phi_{g+1}$, for each $g = 0, \dots, \beta - 1$. We now find a value for l_i which is rounded down to the nearest value in set $\left\{\gamma_0, \dots, \gamma_\beta\right\}$ such that it does not exceed the load of relay node i. To do this, we need to define a binary variable $\tilde{u}_i^g$ that is equal to 1 if $l_i \geq \gamma_g$, and to 0 otherwise for each $i \in R$ and $g \in \{1, 2, \dots, \beta\}$. We represent this relationship by the following forcing constraints:

$$\tilde{u}_i^g \geq \frac{l_i - \gamma_g + 1}{\sum_{b \in B} d_b^s - \gamma_g + 1}, \qquad \forall i \in R, g \in \{1, 2, \dots, \beta\}. \tag{59}$$

Finally, the estimated value of Re_i in the lower bounding model can be obtained as

$$Re_i^L = 1 + \sum_{g=1}^{\beta} \tilde{u}_i^g (\phi_g - \phi_{g-1}). \qquad \forall i \in R, \tag{60}$$

In summary, the lower bounding model includes the objective function given in (25) subject to constraints (2)-(15), (31), (32), (33), (59), (60), and binariness restrictions on the $\tilde{u}$-variables in which variable Re_i is substituted by

variable Re_i^L. Since the value of l_i is rounded down to the nearest value in the set $\{\gamma_0, \dots, \gamma_\beta\}$, the estimated value of Re_i from l_i is an overestimation of the reliability value for each relay i. Therefore, if constraints (31), (32), and (33) are satisfied by reliability value of relay nodes, they should be satisfied by the overestimation reliability value of them as well. Hence, the lower bounding problem is a relaxation of the original problem and can provide a lower bound for this latter.

A similar approach can be applied to find an upper bound for the problem using the underestimated value of Re_i. Hence, the definition of $\tilde{u}_i^g$ should be revised as follow:

$$\tilde{u}_i^g = \begin{cases} 1, & \text{if } l_i > \gamma_g \\ 0, & \text{otherwise,} \end{cases} \qquad \forall i \in R, g \in \{0, \dots, \beta - 1\}.$$

The following forcing constraints can therefore guarantee this relationship.

$$\tilde{u}_i^g \geq \frac{l_i - \gamma_g}{\sum_{b \in B} d_b^s - \gamma_g}, \qquad \forall i \in R, g \in \{0, 1, \dots, \beta - 1\}. \tag{61}$$

and the estimated Re_i-value in the upper bounding model is given as:

$$Re_i^U = 1 + \sum_{g=0}^{\beta-1} \tilde{u}_i^g (F_{\{g+1\}} - F_{\{g\}}), \qquad \forall i \in R. \tag{62}$$

Thus, the upper bounding model is composed of the objective function given in (25) subject to constraints (2)-(15), (31), (32), (33), (61), (62), and binariness restrictions on the $\tilde{u}$-variables in which variable Re_i is substituted by variable Re_i^U.

The lower- and upper-bounding models can be linearized using the same technique presented in Section 4.

6. Cutting plane-based heuristic

In this section, we design an iterative method based on the *cutting plane algorithm* to find an optimal solution for the REAWD problem by adding valid cuts to the lower-bounding formulation presented in Section 5.
We first formulate the lower bounding model using subsets $\{\gamma_0, \dots, \gamma_\beta\}$ and $\{\phi_0, \dots, \phi_\beta\}$ and find an integer-feasible solution, $(\hat{y}, \hat{x}, \hat{z}, \hat{f})$ for it using the branch-and-bound method [46]. We then compute the load and reliability of each relay node using constraints (14) and (16), respectively, and calculate the path reliability of each biosensor $b \in B$. Since the lower bounding problem is a relaxation of the REAWD problem, we check which path is a reliable path.

Let us define $\bar{B} \subseteq B$ as a set of all violated biosensors, that is the set of all biosensors for which the path reliability is less than a given threshold τ^b. If $\bar{B} = \emptyset$, it means that we have no violated biosensor, hence we found a feasible solution for the REAWD problem. Otherwise, if $\bar{B} \neq \emptyset$, we cut off the current solution using the valid inequality proposed in Subsection 6.1. To improve the speed of convergence and the quality of the initial valid inequalities, a warm-start strategy is presented in Subsection 6.2 as well. An algorithmic implementation of our method is presented in Algorithm 1.

6.1. Valid inequality

Let us assume that we could not find a reliable path for some biosensors, i.e., $\bar{B} \neq \emptyset$. In this case, we should generate a valid inequality to cut off the current solution from the feasibility region of the lower bounding problem and revise violated paths. A violated path can be modified using at least one of the following statements:

- Change the transmission path from biosensor $b \in \bar{B}$ to the sink.
- Reduce the load of relay nodes visited in the violating path.

For this purpose, we define sets I_b and $\tilde{I}_b$ as follows:

$$I_b = \left\{ (i, j, b') \,|(i, j) \in \hat{A},\ j \in p_b,\ b' \in B,\ \hat{z}_{ij}^{b'} = 1 \right\},$$

$$\tilde{I}_b = \left\{ (b, i), (i, s) \in \tilde{A} |\ i \in p_b,\ b \in \bar{B},\ \hat{x}_{bi} = 1 \text{ or } \hat{f}_{is}^b = 1 \right\},$$

where p_b is the set of relay nodes that lay on the transmission path for $b \in \bar{B}$. In particular, I_b is the set of all incoming arcs to relay nodes in p_b whose corresponding z-variables are equal to 1 in the current solution and $\tilde{I}_b$ is the set of all assigned pairs of the form (biosensor, relay) or (relay, sink) for each relay node in p_b in the current solution. To modify a violated path, the value of at least one of the variables z^b_{ij}, x_{bi} or f^b_{is} should be changed to zero in the current solution. This constraint is represented as follows:

$$\sum_{(i,j,b')\in I_b} (1 - z^b_{ij}) + \sum_{(b,i)\in \tilde{I}_b} (1 - x_{bi}) + \sum_{(i,s)\in \tilde{I}_b} (1 - f^b_{is}) \geq 1. \tag{63}$$

We now show that inequality (63) is a valid inequality and cuts off the current solution. Assume that for an arbitrary solution, the left-hand-side of (63) is equal to zero. Hence, biosensor b uses the same transmission path as before and the load on every relay in p_b is at least as large as it was in the previous solution. This result shows that biosensor b is a violating biosensor and consequently this solution is an infeasible solution for the problem. Since in the current solution the left-hand-side of (63) evaluates to zero, the current solution is an infeasible solution and inequality (63) cuts off it.

6.2. Warm-start strategy

Our algorithm suffers from slow convergence due to the generation of low-quality valid inequalities in initial iterations. To overcome this drawback, we propose a warm-start strategy to generate an initial set of tight cuts.

To perform data routing in WBANs, we need to ensure that all data are delivered from each biosensor to the sink. Then, we should guarantee the existence of one connecting path with sufficient capacity from each biosensor to the sink. This implies that if an arc $(i, j) \in \hat{A}$ is used to ship data that enters some relay node $i \in R$, then one arc that exits from the same node i must be used to transfer data, and vice versa. We represent these conditions as follows:

$$z^b_{ij} \leq \sum_{h\in RS(i)} z^b_{hi}, \qquad \forall b \in B, i \in R, j \in FS(i), \tag{64}$$

$$z^b_{ji} \leq \sum_{h\in FS(i)} z^b_{ih}, \qquad \forall b \in B, i \in R, j \in RS(i). \tag{65}$$

Similarly, this condition should be imposed on biosensors and the sink node to ensure the connectivity between biosensors and relays, and between relays and the sink as well.

$$x_{bi} \leq \sum_{h\in FS(i)} z^b_{ih}, \qquad \forall b \in B, i \in \widetilde{FS}(b), \tag{66}$$

$$x_{is} \leq \sum_{h\in RS(i)} z^b_{hi}, \qquad \forall b \in B, i \in \widetilde{RS}(s). \tag{67}$$

On the other hand, each relay which can establish direct links with biosensors or the sink should possess enough capacity. Therefore, for each relay $i \in \tilde{FS}(b)$ and $i \in \tilde{RS}(s)$, we added the following cover cuts:

$$\sum_{b\in B} d^b x_{bi} \leq v_i, \qquad \forall i \in \widetilde{FS}(b), \tag{68}$$

$$\sum_{b\in B} d^b x_{is} \leq v_i, \qquad \forall i \in \widetilde{RS}(s). \tag{69}$$

Algorithm 1 Cutting plane algorithm-based heuristic for the REAWD problem

Input: Set parameters E_{TXelec}, E_{amp}, E_{RXelec}, D_{ij}, CR, U, a_{bi}, e_{is}, v_i, c_j, n_{ij}, t_s^b, $\bar{B} = \emptyset$, ϵ, $LB = -\infty$, $UB = \infty$
Output: Optimal Reliable Design of Energy-efficient Wireless Body Area Networks

Formulate the lower and upper bounding models using subsets $\{\gamma_0, \ldots, \gamma_\beta\}$ and $\{\phi_0, \ldots, \phi_\beta\}$
Add initial set of tight cuts (64)-(67), and (68)-(69) to the lower and upper bounding models
WHILE $UB - LB \geq \epsilon$
Let LB and UB be the objective values of the integer-feasible solutions obtained respectively from the lower and upper bounding models using branch-and-bound method
for each $i \in R$ **do**
    Calculate $\hat{l}_i$ and $\hat{Re}_i$ using constraints (14) and (16), respectively
end for
Set $\bar{B} = \emptyset$
for each $b \in B$ **do**
    if $\left(\sum_{i \in \tilde{FS}(b)} \hat{Re}_i \hat{x}_{bi}\right) \prod_{(i,j) \in \hat{A}} (\hat{Re}_i)^{\hat{z}_{ij}^b} < t_s^b$ **then**
        Update $\bar{B}$ by setting $\bar{B} = \bar{B} \cup \{b\}$
    end if
end for
if $\bar{B} = \emptyset$ **then**
    Return LB, UB, and obtained feasible solution
    else
    for each $b \in \bar{B}$ **do**
        Add valid inequality (63) to lower and upper bounding models
    end for
end if
END WHILE

7. Wireless Body Area Network Scenario

In this study, we consider a normal standing scenario with arms hanging along each side, as shown in Figure 1. This topology contains a complete WBAN scenario with quite a high number (exactly 13) and the most different types of biosensors; each of them is deployed in a fixed place to sense and gather biomedical data according to (x, y) coordinates, as presented in Table 5. The sink device is deployed in the origin of the coordinate system. The Euclidean distance (in meters) between biosensors and the sink for the single-hop case, and between biosensors and the nearest node for the multi-hop case are reported in Table 5 as well. Similarly to [44], we identify eight ellipsoidal regions for relay positioning and establishing a multi-hop communication in the WBAN, as shown in Figure 4, in which relays can be installed uniformly at random on the body surface or patient's clothes. The identification of these regions is based on the patient's body posture, which may make changes in relay node installation location and wireless communication channel (and as a consequence, on the network topology). Indeed, we consider general regions for each body posture. These areas cover the patient's entire body and allow nodes to establish wireless communications with each other without impairing body movement. We consider 2D virtual coordinates for these areas, similarly to the virtual coordinates used in [44]. To protect the heat-sensitive tissue of the body against the heat released by the network devices [17, 33, 47], reducing interference [16], and decreasing energy consumption [47], we are required to decrease the transmission power of the devices and thus decrease the communication range between them. When we are dealing with wireless communication around the human body, we also need to consider the effects of specific absorption rate and heating of the wireless devices on the human body. The specific absorption rate (SAR) is defined as a measure of the amount of radio frequency energy absorbed by human tissue in units of mass [48]. When the distance between biosensors and the sink is large, we need a high transmit power for the antenna to ensure packet delivery; this in turn leads to increase the heat generated by biosensors and then the SAR level. Hence, we should maintain the value of SAR within a threshold level. In this paper, we adjust the distance between biosensor nodes and the sink using relay nodes so that biosensor nodes can complete their transmissions within the distance using a low transmission power. Hence, Multi-Hop communication can decrease the negative impact of SAR and improve

Parameter	Value
E_{TXelec}	16.7 (nJ/bit)
E_{RXelec}	36.1 (nJ/bit)
$E_{amp}(3.38)$	1.97 (nJ/bit)
$E_{amp}(5.9)$	7990 (nJ/bit)
Frequency range	2.4 – 2.45 GHz

Table 4
Energy consumption values and frequency range for the Nordic nRF2401 transceiver.

Biosensor	A	B	C	D	E	F	G	H	I	J	K	L	M	sink
x-coordinate (m)	0.10	-0.20	-0.03	0.05	0.10	-0.10	-0.10	0.10	-0.10	-0.05	0	0.20	0.10	0
y-coordinate (m)	-0.60	-0.10	0.10	0.25	-0.90	-0.30	0.35	0.35	0.60	0	0.70	-0.20	0.90	0
Single-hop (m)	0.66	0.13	0.14	0.47	0.85	0.23	0.53	0.53	0.66	0.3	0.8	0.31	0.85	-
Multi-hop (m)	0.66	0.13	0.14	0.47	0.2	0.17	0.36	0.07	0.45	0.48	0.37	0.58	0.2	-

Table 5
Deployment of biosensors on patient's body. Distances (in meters) between biosensors and the sink for the single-hop case, and between biosensors and the nearest node for the multi-hop case.

transmission success rate simultaneously [48, 49]. To do this, we set connectivity parameters a_{bi} and e_{is} to one only if a relay node i is deployed on a radius not greater than CR cm (Communication Range) from the biosensor b and the sink node s, respectively. To evaluate the effect of the communication range between relay nodes on the total energy consumption and the total number of installed relays, we consider two different values for the connectivity parameter between relay nodes, i.e., $CR = 30$ and $CR = 90$ cm [44, 17]. The installation cost and the maximum capacity of relay nodes are assumed to be equal to 10 monetary units and 250 kb/s, respectively [17].
The reliability function proposed in this work is based on the total incoming load in relay nodes, i.e., Re_i=F(l_i), which must be a non-increasing, concave, and continuous function. Therefore, the reliability function Re_i can be customized depending on the used sensors and communication technology. Through this assumptions, the function defined by Equation 1 will be used as the reliability function (we rewrite it here for ease of readability):

$$Re_i = 1 - \frac{{l_i}^2}{{v_i}^2}. \tag{70}$$

As for the wireless channel propagation model, the path loss exponent is considered in [15] equal to 2 for free space propagation and about 4 in a lossy environment. However, the value of the path loss exponent can be larger than 4 near the human body. Elias [17] shows that this value is in the range of 5 to 7.4. More specifically, it is about 3.38 (at the lowest level) in the line of sight case (when transmissions take place on the same side of the body), and 5.9 when propagation is around the body (non-line of sight case) [17]. To calculate energy consumption, we use the parameters corresponding to the Nordic nRF2401 transceiver [50] in the 2.4-2.45 GHz frequency range, which is commonly used in body sensor networks [43, 17, 30]. Table 4 reports the energies values and the frequency range for the Nordic nRF2401 transceiver considered in our work. Thus, the radio dissipates $E_{TXelec} = 16.7$, $E_{RXelec} = 36.1$ to run the transmitter and receiver circuitry, respectively. By limiting the devices' communication range and decreasing the transmission power, we should use a transmission amplifier to deal with the weakness of signals and handle the flow carrier signals to other devices [51]. The transmission amplifier $E_{amp}(n_{ij})$ depends on the path loss value n_{ij}, it is equal to 1.97 nJ/bit for $n_{ij} = 3.38$ (LOS) and 7.99 nJ/bit for $n_{ij} = 5.9$ (NLOS).

8. Numerical Results

In this section, we evaluate and compare the performance of the proposed model and algorithm. Hence, we consider the proposed model in the following two versions. The first version is defined by getting the objective function (25) and constraints (7)-(13) and (2)-(6). This model is called "*Model A (No-Reliability)*", which can address both the relay positioning and the data routing problems in a way that leads to minimizing the number of installed relays and the total energy consumed by the network without considering reliability constraints. This model does not prevent congestion occurrence, and as a consequence, the chosen paths might be unreliable. The second version of the

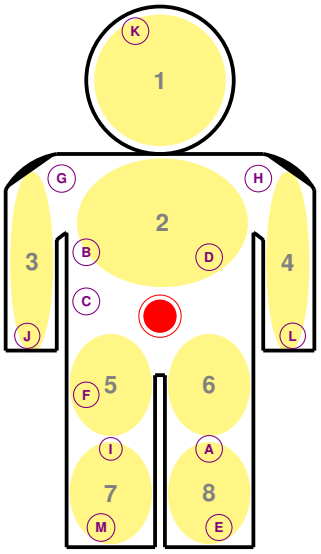

Figure 4: A wireless body area network with different areas for installing relays.

proposed model is given by the linear model derived from the proposed non-linear one, which includes the objective function (25) and constraints (7)-(12), (13), (2)-(6), and (42)-(58). This model is called "*Model B (Full-Model)*". In addition to minimizing the cost of installing relays and network energy consumption, Model B can control congestion in the network and then data will be transmitted to the sink through reliable paths.

We consider four cases to evaluate the performance of the proposed models as follows:

- In the first evaluation, we explore the sensitivity of models A and B to the number of relays allowed to be installed in the network (U) in Section 8.1, data rate (d) in Section 8.2, and the weighting parameter (α) in Section 8.3.
- In the second evaluation, we examine the effect of the threshold probability parameter (τ) on energy consumption, data routing, number of installed relays, the reliability function, and the amount of load on relay nodes, as well as the path reliability in Section 8.4.
- In the third evaluation, we compare the performance of the proposed model in Section 8.5 to existing methods in terms of reliability, energy consumption, and the number of installed relays.
- In the fourth evaluation, we evaluate the computational efficiency of our cutting-plane algorithms for solving the REAWD problem in Section 8.6.

The following metrics are used to measure the effectiveness of the approaches considered in our numerical analysis, as well as to compare their performance:

- E_{tot}: Total energy consumed by WBAN devices.
- E_{tot_R}: Total energy consumed by installed relay nodes in the network.
- E_s: Energy consumed by each biosensor to transfer sensed data.
- E_R: Energy consumed by each installed relay.
- N_R: Number of installed relays.
- Re^{path}_{min}: Minimum path reliability among all biosensors to the sink.
- Re^{path}: Reliability of data transmission path from each biosensor to the sink.

- V_{min}: Minimum remaining capacity of a set of installed relays.
- Time: Computation time to obtain the optimal solution (in seconds).
- Gap(%): The relative optimality gap is defined as the relative distance between the objective function value of an approximate solution and an optimal objective function value.

The results reported below are the optimal solutions of the model instances that have been implemented in the GAMS software[1], a mathematical programming modeling language, and solving them with CPLEX 11, a mathematical programming solver. For each network scenario, the reported results have been obtained averaging each point on 10 instances. All computations are executed on a Core-i7/4GHz/16GB system.

8.1. Effect of the number of candidate sites for relays installation (U)

Increasing the candidate sites for installing relays can completely affect reducing network energy consumption and also increase the complexity of the network by raising computation time. We evaluate the effect of increasing the number of candidate sites available for relay installation, varying the U parameter from 40 to 200 in the network, on the performance of Models A and B with two different relay communication ranges ($CR = 30$ and $CR = 90\ cm$). Please note that, as can be observed in the Tables and Figures hereafter, the number of relays actually installed by our model is small (less than 5 and 7 with communications ranges equal to 90 and 30 cm, respectively).

Table 6 shows the average values of the total energy consumed by the network (E_{tot}), the energy consumed by each relay (E_R), the number of installed relays in the network (N_R) and the computation time for Models A and B, while each biosensor transfers a unit of data. Since all biosensors have a reliable transmission for a unit of data due to reliability function features (relay capacity dependence), all metrics for Model A and B have the same value (i.e., reliability constraints are effect-less in this circumstance), except for the computation time outlined in Table 6. According to Figure 5, increasing parameter U decreases the total energy consumption of the network and relays. Since each model addresses the optimal relay positioning problem, the relays are optimally deployed on the patient body with a communication range of $CR = 90\ cm$, since there is less limitation for relays with this communication range. Thus the average energy consumption of the whole network in the case of $CR = 90\ cm$ is less than the case where $CR = 30\ cm$. However, increasing the communication range of relays is always faced with some benefits and drawbacks. As can be seen in Table 6, on the one hand setting $CR = 90$ cm, our models are into using the least number of relays and constantly install three relays for different values of U, which means biosensors transfer their data through common relays. Subsequently, relays installation cost and total network energy consumption would decrease due to installing relays in the most optimal places. On the other side, the probability of congestion occurring, in this case, rises due to reducing the number of the installed relay by $CR = 90$ cm. Moreover, the energy consumption by the relays is approximately twice as much as in the case where $CR = 30\ cm$ that would threaten relays surviving and leads to shortened the network lifetime. Therefore, by considering $CR = 30\ cm$, in addition to minimizing the network energy consumption and increasing its lifetime, the probability of congestion occurrence in the network is also reduced.

Time is another metric that has been calculated for two models A and B with two different communication ranges $CR = 30$ and $CR = 90$, then its result is depicted in figure 6. This metric has been defined as the computation time needed to reach the optimal solution in both models. Comparing these values, there is a large gap between the computation time for model A and model B. The optimal solution in model A can be achieved in under 1 second for $U = 40$ and remain below 25 seconds for $U = 200$ when $CR = 30$ cm the value then increased from 1.008(s) to less than 50 seconds by setting $CR = 90$. Subsequently, all computation for solving model A and achieving optimal solution takes less than one minute, on average, while the computation time increases consistently for model B. It takes lower 28 seconds for model B to obtain an optimal solution when $U = 40$ and $CR = 30$. This value then steadily increases up to 7 minutes for $U = 100$, and it aggressively goes up by increasing U values. One noticeable point regarding the communication range of $CR = 90$ cm is rising network complexity due to increasing the established links between relays. This fact is detected in figure 6, which compares the computational time needed to obtain the optimal solution for model A and model B. We can see that the computation time for solving models, in this case, is at least two times higher than the case $CR = 30$. Model B needs at least 2 minutes to fulfill an optimal solution when $U = 40$ and more than 8 hours for the case where $U = 200$.

[1] https://www.gams.com/

U	CR=30 (cm)					CR=90 (cm)				
	$E_{tot}\ (nJ/bit)$	$E_R\ (nJ/bit)$	N_R	Time(s)/A	Time(s)/B	$E_{tot}\ (nJ/bit)$	$E_R\ (nJ/bit)$	N_R	Time(s)/A	Time(s)/B
40	1473	121	6.9	0.910	27.246	906.744	229.822	3	1.008	121.104
50	1436	111	7.2	1.343	55.068	906.621	229.794	3	3.635	250.958
60	1420	114	6.8	1.804	92.62	906.183	229.647	3	3.847	368.706
80	1394	113	6.8	3.307	211.654	906.04	229.599	3	7.688	830.618
100	1353	110	6.8	4.852	428.066	906.035	229.598	3	11.111	1529.496
150	1331	102	6.8	11.769	2184.285	905.929	229.565	3	14.636	9894.618
200	1304	98	7	23.820	8277.377	905.77	229.506	3	48.121	32464.982

Table 6
WBAN scenario: Total energy per bit consumed by (1) the whole network and (2) each relay, (3) the number of relays installed in the WBAN, (4) and (5) computation time (in average), obtained with Model A and B, varying number U of candidate sites

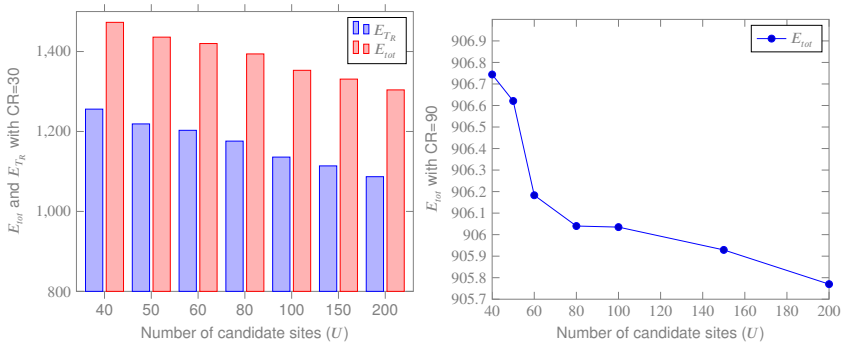

Figure 5: Total energy consumed by the whole network (E_{tot}) and by relays (E_{T_R}) in Model A, with CR=30 and CR=90 cm.

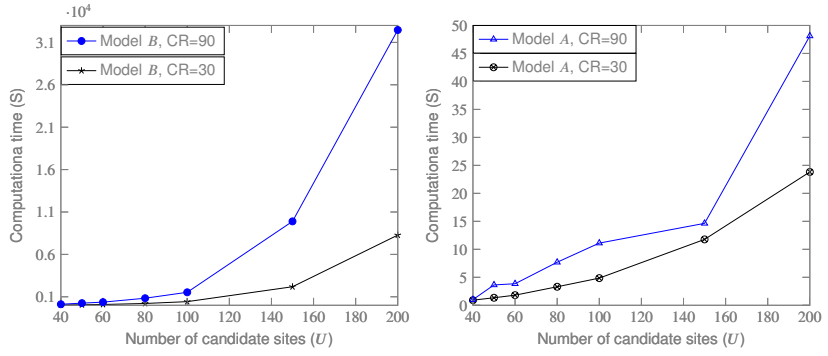

Figure 6: Computation time to obtain optimal solutions as a function of the number of candidate sites (U).

It is worth mentioning that wireless body area network technology is scalable for small-scale arrangements in practice [52]. Hence, the number of relays allowed for installation, as well as the candidate sites [17], is in general small, and therefore U values are expected to be way less than 80. On these candidate sites, only a handful of relays is installed, as can be seen in the numerical results. Hence, the computation time required to obtain the optimal solution will always be short in practical network scenarios (model A and model B take less than 7 (s) and 830.618 (s) to compute optimal solutions, respectively).

Metrics	$d_s^b = 30$				$d_s^b = 50$				$d_s^b = 70$			
	A	B_{τ_1}	B_{τ_2}	B_{τ_3}	A	B_{τ_1}	B_{τ_2}	B_{τ_3}	A	B_{τ_1}	B_{τ_2}	B_{τ_3}
$E_{tot}(mJ/bit)$	41.85	41.851	40.108	40.848	70.278	70.542	70.278	66.321	100.977	102.084	100.238	100.24
N_R	13.4	13.4	13.6	13.3	14.5	14	15	15	14.8	16	17	23
V_{min} (kb)	130	130	130	130	0	100	100	150	40	110	110	180
Re_{min}^{path}	0.516	0.516	0.683	0.725	0	0.41	0.538	0.706	0.059	0.323	0.583	0.783

Table 7
WBAN scenario (with $CR = 30\ cm$): (1)Total energy per bit consumed by the whole network, (2) number of relays installed in the WBAN (on average), (3) minimum remaining capacity of a set of installed relays, and (4) minimum path reliability among all biosensors to the sink paths obtained with Models A and B (B_τ), varying d_b^s and τ_1= 0.3, τ_2=0.5, τ_3=0.7

8.2. Effect of the traffic demand (d)

Increasing the rate of data offered by the biosensor may lead to network congestion, hence a careful traffic distribution must be performed in the network in a balanced manner. In this section, we compare the functionality of Models A and B by investigating the effect of increasing the data rate on the total network energy consumption (E_{tot}), the energy consumed by each relay (E_R), the number of installed relays (N_R), the minimum remaining capacity of the set of the installed relays (V_{min}), the minimum path reliability among all biosensors to the sink (Re_{min}^{path}) and how the traffic is distributed in the network to control or prevent congestion occurrence. To do this, we increase the traffic gradually from $d^b = 30\ kb/s$ to $d^b = 70\ kb/s$, and consider three different values for the threshold probability parameter, namely τ^b=0.3, τ^b=0.5, and τ^b=0.7 $\forall b \in B$ while U=100.

Table 7 shows the values of the mentioned metrics. Through this table, as expected, increasing the data rate would increase the network energy consumption for both models. And also, when the data rate increases in the network, Model A could not handle the huge traffic generated by biosensors and just route them to other devices without considering their congestion level. In this case, some relays receive or transmit a large amount of traffic, with respect to their capacity, and therefore such relays will run out of capacity and will not be available for further communication activity (transmission or reception). Furthermore, if relays are deployed within some biosensors or the sink's communication ranges whose remaining capacity is at a low level or depleted, biosensors will not be able to transfer their data to these relays or they will be unable to deliver their data to the sink through them. That is, there will be no reliable path for some biosensors to transfer their data to the sink. In both cases, patient monitoring may be interrupted, congestion will occur in the network, along with increased packet losses and delays, thus creating critical situations from the medical point of view. For example, when d^b increases from 30 to 50 kb/s, V_{min} dropped suddenly from 130 kb/s to 0 and as a result, some paths from biosensors to the sink which pass through these relays became completely unreliable due to the too low value of Re_{min}^{path} achieved for d_b^s=50 in Model A. Adjusting the threshold parameter in Model B leads to managing data routing and decreasing the traffic passing through each relay. This issue is illustrated in Table 7, in which increasing the threshold probability parameter τ^b leads to increasing the Re_{min}^{path} value. Although increasing the threshold probability parameter increases the number of installed relays in the network, this action leads to decreasing the total energy consumption in the network, which in turns contributes to increasing the network lifetime as well.

8.3. Effect of the weighting parameter (α)

As we can see, our proposed model is a bi-objective model, which is reduced to a single-objective model by associating a weighting parameter α. Hence, we now assess the performance of Model A based on the objective function terms. To check the importance of the role of the weighting parameter (α) in minimizing network energy consumption and relay install cost, we vary the value of α from zero to ∞ and compute results on the topology depicted in Figure 1. Table 8 shows the objective function value for our model in the WBAN scenario depicted in the above figure as a function of the weighting parameter α. It should be noted that setting $\alpha = 0$ in our model just minimizes the relay installation cost without considering energy consumption of biosensors and relay nodes, while with $\alpha \to \infty$ our model minimizes the energy consumption of biosensors and relay nodes without considering the installation cost of relay nodes.

We therefore consider three cases. In the first and second one, we just take one term of the objective function,

α	E_{tot}	C_{IR}
0	1.66	63
10^0	1.326	82
10^1	1.279	86
10^2	1.273	110
10^3	1.22	110
10^5	1.281	136
10^{10}	1.447	140
10^{15}	1.447	145

Table 8
Total energy consumed by the whole network and total installation cost as a function of the weighting parameter (α)

i.e., minimizing network energy consumption or minimizing the cost of installing relays, respectively. In the third case, we consider the cost of installing relays and energy consumption simultaneously and evaluate the impact of the weighting parameter α on the solution of the proposed model. In the $\alpha = 0$ scenario, our model installs a minimum number of relays, $N_R = 6.3$, with high energy consumption, which is about $E_{tot} = 1.66(\mu J/bit)$. When Model A just minimizes the overall network energy consumption, neglecting the relay install cost, i.e., when $\alpha \to \infty$, it uses a higher number of relays to minimize the network energy consumption. As illustrated in Table 8, the average value of N_R in such case is equal to 14.5. We can note that the WBAN installation cost increases from 63 to 145, a 54% increase. Hence, considering only one of the two terms in the objective function increases the network energy consumption or installs an extra, unnecessary number of relays in the network, which makes disturbance on the patient comfort and movement. Thus, to strike a balance between the energy consumption and the number of relays installed in the network, we adjusted the considered weighting parameter to minimize both relay install cost and network energy consumption. In this case, by increasing α as is shown in Table 8, the cost of installing relays increases sharply, while the amount of network energy consumption decreases firstly (from $\alpha = 0$ to 10^3), then has an increasing trend and finally becomes leveled off. Therefore, by adjusting α, the model can prevent installing unnecessary relays, which can protect sensitive organs of the body against the heat and radio frequencies released by the relays, and at the same time decrease the network energy consumption, thus increasing the WBAN's lifetime. In particular, for $\alpha = 10^3$, the WBAN energy consumption is about 1.220 ($\mu J/bit$) per bit, which means more than 34 and 22% reduction compared to the case $\alpha = 0$ and $\alpha = \infty$, respectively. At the same time, such α value reduces the installation cost (more than 24%) compared to the $\alpha \to \infty$ case.

8.4. Effect of threshold probability parameter (τ)

In this section, various amount of threshold probability parameter is considered to analyze the functionality of model B in (i) data routing, (ii) the number of the installed relay, and (iii) energy consumed by the network.

To achieve an effective result of increasing the threshold probability parameter, τ, we first need to determine an initial value for that. We calculate the value of the reliability of biosensors in transferring data to sink in model A in which each biosensor generates d^b=45 kb and candidate sites $U = 80$. The lowest path reliability value is selected as an initial threshold parameter, which is $\tau_0 = 0.419$ in our scenario. We hence choose different values for τ^b varying from 0.419 to 0.8. Figure 7 illustrates the data routing from biosensors to the sink for two different probability threshold parameters, 0.419 and 0.8, with $U = 80$. As can be seen from this figure, for a probability threshold parameter equal to 0.419, the biosensors transfer their data towards the sink through common relays and select the shortest path mainly in terms of energy consumption to reach the sink. By increasing the threshold probability parameter (τ^b), the biosensors attempt to send their data towards the sink following disjoint relay node paths. This is due to the fact that adjusting the threshold probability parameter reduces congestion and as a consequence the incoming traffic on relay nodes. Therefore, to satisfy the threshold probability parameter, the number of installed relays (N_R) will increase, as it can be seen in Figure 8. Note that when $\tau^b = 0.8$, we observe that only biosensors far from the sink have more than one relay in their data transmission path and other biosensors transfer their data to the sink through only one relay. In addition, biosensors use the most diverse relays to transfer their data to the sink. This reduction in the number of relays within the data transmission path for each biosensor is due to the need of satisfying the fixed threshold, and since each biosensor uses the minimum number of relays to transmit its data to the sink, the energy consumed by the network may increase (according to the number of deployed relays on each path); this is the cost of having more

reliable routes. In other words, biosensors' data transition path reliability constraints decrease the incoming traffic to each relay, and the level of this reduction depends on the value of the threshold probability parameter. To satisfy this value, the number of installed relays (NR) will increase, as can be seen in Figure 8.
In Figure 7 (a), some biosensors, such as E and L, have completely reliable paths to transfer their data to the sink since they have disjoint relay node paths (with path reliability larger than 0.8), and some other biosensors like D and K are at risk of congestion and have minimum path reliability. However, when the threshold probability parameter increases, the path reliability of all biosensors will be balanced. This is due to the balancing effect, and the distribution of traffic that comes with it, with congestion reduction at some relays, as a result of applying reliability constraints. Table 9

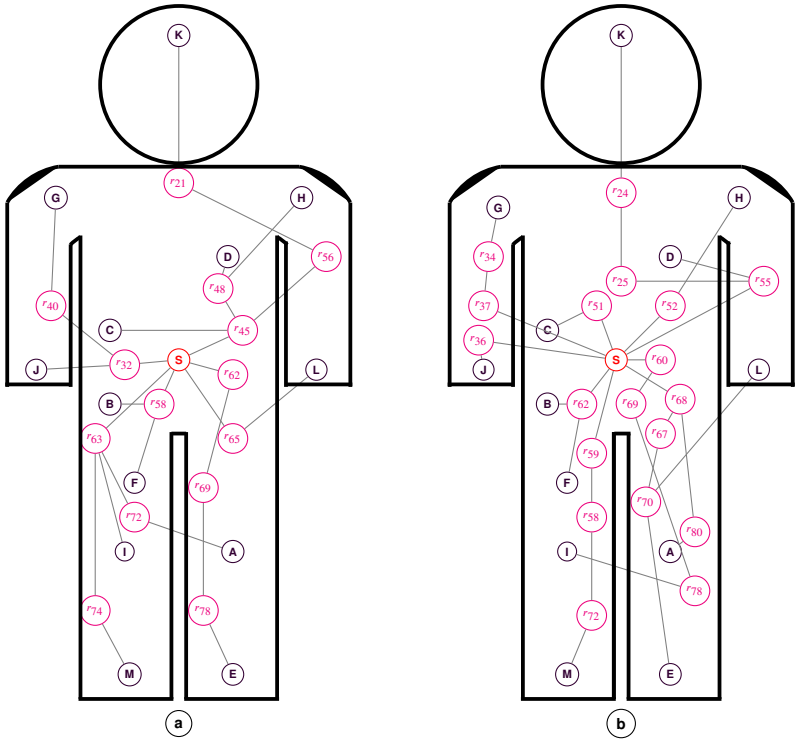

Figure 7: Routing changes by increasing the probability threshold parameter from (a) τ^b=0.419 to (b) τ^b=0.8.

reports the mean, variance, standard deviations, the minimum and maximum values for the load passing through relay nodes and their reliability, balancing the traffic passing them, as a result of the increased threshold probability parameter. This table illustrates the decrease in both the mean and maximum values for the traffic load that passes through relays, which prevents node-level congestion and leads to having completely reliable nodes and paths. For example, Figure 7(a) shows that 31% and 23% of the total traffic generated by the biosensors is transmitted to the sink through r_{45} and r_{63}, respectively. Since these relays have direct communication with the sink, high-volume data transmissions by them may deplete their battery power sources. As a result, data may be delayed in reaching the sink, or if some nodes die, the communication between relays and the sink would be interrupted.

On the other hand, increasing the probability threshold parameter permits to restrict the number of relays that receive high traffic volumes from other nodes; this can be observed in Figure 7(b): when τ^b=0.8, each biosensor tries to transfer its data through individual paths, therefore the load passing through each relay decreases and most of the relays transfer a lower amount of traffic to other relays or the sink. We now investigate the impact of the threshold parameter on the total energy consumed by the network and the number of installed relays by varying τ^b on a wider range, i.e., from 0.1 to 0.8. Figure 8 illustrates the changes in both the energy and number of installed relays as a function of the threshold parameter. At first, we solve Model A for the scenario with $U = 80$ and $d = 45$ kb/s. In this case, the total energy consumed, the average number of installed relays, and the minimum path reliability are 63.489 ($\mu J/bit$), 14.7, and 0.419, respectively. Then, we solve Model B, varying the threshold parameter from 0.1 to 0.8. From Figure 8, we observe that by increasing τ^b, the average number of installed relays increases. Hence, increasing

τ	Mean		Var		Std		Min		Max	
	l_i	Re_i	l_i	Re_i	l_i	Re_i	l_i	Re_i	l_i	Re_i
0.419	73.9	0.88	1746.8	0.019	41.7	0.138	45	0.481	180	0.967
0.5	72	0.9	1099.2	0.008	33.1	0.09	45	0.708	135	0.967
0.6	61.8	0.92	1046.2	0.008	28.7	0.08	45	0.708	135	0.967
0.7	69	0.91	829.2	0.005	28.7	0.07	45	0.708	135	0.967
0.8	54.4	0.94	355.2	0.002	18.8	0.04	45	0.87	90	0.967

Table 9
Effect of the threshold probability parameter (τ) on path reliability

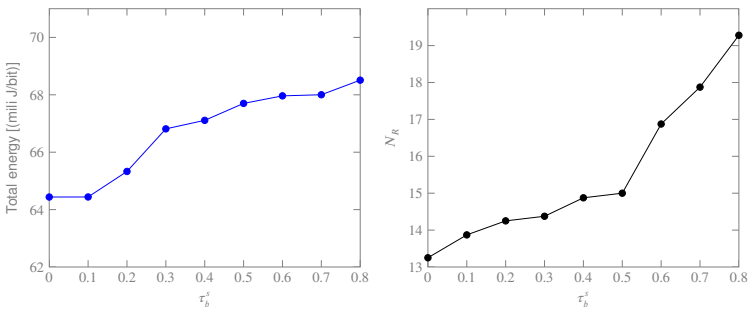

Figure 8: Effects of increasing the probability threshold parameters on the network energy consumption and the number of installed relays.

the threshold parameter forces the biosensors to change high-congestion paths and select distinct relays to transmit data towards the sink. In this way, the number of relays deployed in the data transmission path of each biosensor decreases, and as a result the distance between devices increases as well. Therefore, the energy consumed by the network increases. In general, the network energy consumption depends on the number of relays deployed in each data transmission path from a biosensor to the sink, and applying path reliability constraints, even with high threshold parameters, does not have a significant impact on increasing the network energy consumption.

8.5. Comparison with existing approaches

The purpose of this subsection is to compare the proposed model with other notable models proposed in the literature [15, 17, 18, 30] for minimizing network energy consumption. This comparison is done in terms of both energy consumption and transmission reliability. Therefore, we first perform a comparative study with other models, solving Model A, in terms of network energy consumption minimization, and then Model B in terms of path reliability for each biosensor. For this comparison, we measure the performance obtained by existing methods in the same scenario illustrated in Figure 4. Table 10 reports the average value of the total energy (E_{tot}), the energy consumed by each biosensor (E_s), and the number of relays installed in the WBAN (N_R), using our proposed model ($U = 200$, $CR = 30$ and 90) and under the EAWD model (with $p = 200$, $CR = 30$ and 90), the single-hop, multi-hop and relay network approach.

As shown in Table 10, Model A has a better performance with respect to the single-hop and multi-hop methods in terms of the total energy consumption and the energy consumed by each biosensor. Because it determines the optimal location for the relays and uses them as intermediate nodes. Indeed, E_{tot} and E_s in the scenario with $U = 200$ and $CR = 30$ exhibit, respectively 87.4% and 97.9% reduction with the proposed Model A compared to the single-hop method, and 59% and 93% reduction if compared to the multi-hop sensor-based method, while only seven relays (on average) are installed in the network. In addition, if we vary the relay communication range from 30 to 90 cm, we observe a more consistent reduction in the network energy consumption, down to 0.906 ($\mu J/bit$), as well as in the number of installed relays (on average 3). Hence, using Model A consistently increases the WBAN's lifetime

compared to the single-hop and multi-hop sensor-based methods. In the hPSOSA-S2 method, the network's total energy consumption, with a tiny difference, is almost equal to the network's energy consumption in model A (for the case $CR = 30$). however, this method does not guarantee the longevity of the network. Since, except for a small group of biosensors that are deployed at the farthest distance from the sink that can use relays as intermediate nodes, other biosensors use direct communication to transfer data. Therefore, the average energy consumed by each biosensor is at a higher level than the value achieved by our proposed method. In other words, the energy consumed by biosensors in the hPSOSA-S2 method is at least 73.44 percent higher than the reported result by our proposed method.
Table 10 shows that the total energy consumption in the relay network approach is lower than in our model. However, the number of relays in such an approach is predetermined, and 14 relays are installed to minimize the WBAN's energy consumption, while in our model the average of N_R is 3. The free and unrestricted mobility of patients during monitoring is one of the key elements that we further consider in this work, along with motion, which is another important feature of wireless body area networks [43]; hence, the relay network approach can be inefficient in larger scenarios, because it tends to install a larger number of relays in the network, thus possibly impairing patients' movements [17].
Table 11 shows the path reliability from biosensors to the sink in the WBAN topology of Figure 4 for the multi-hop sensor-base and relay-base approach, EAWD, the relay network approach, and the proposed Model B, while Table 12 reports three indexes: minimum, average, and maximum path reliability.
Since the single-hop approach is not, in general, a reliable method due to the direct transfer of data and the large distance between the biosensors and the sink, Model B is compared with the other approaches considered before, except for the single-hop approach.
In previous sections, we have seen that adjusting the threshold probability parameter in model B leads to compute reliable paths from biosensors to the sink, regardless of how far the biosensor is installed from the sink. In the relay network method, biosensors forward their data through predetermined paths; these paths are reliable, in general, but if a relay fails or runs out of capacity/energy, there is no other path to send data through, and this may cause problems in the detection of life-critical emergencies, such as heart attacks or sudden falls.
As seen in Table 12, we can observe that path reliabilities for all biosensors are not uniform in the multi-hop method, and 54% of biosensors' path reliability is, in fact, lower than 0.3; overall, the average reliability value for this method is 0.369. On the other hand, the input traffic to some biosensors, such as D and B, is high; in fact, 90% and 70% of the capacity of biosensors D and B is used to transfer data towards the sink, respectively. Therefore, the successful transmission probability for such biosensors is very low (for D it is equal to (0.16)). In the multi-hop relay-based method presented in [18], only biosensors located at a great distance from the sink can transfer their sensed data using a relay. This method adopts a combination of multi-hop and single-hop approaches, and is not promising in reducing energy and providing at the same time reliable end-to-end paths. This can cause problems, since an early termination of one or more sensors can result in an early termination of the patient monitoring activity.
As observed in Table 10, the total energy consumption in the EAWD model is lower than that in Model A, but this method exhibits weak performance in terms of transmission path reliability. Since these biosensors share important medical data with the physician through the sink (for example, node D could send electrocardiogram information), congestion occurrence, which may happen in the EAWD model, can lead to packet loss or may delay the transfer of data to the sink, and this may cause serious consequences to the patient. However, the EAWD model can find alternative paths if a limited capacity relay is located in the transmission path, but it may spend much energy re-sending data to another relay.

8.6. Analysis of the proposed algorithm

In this section, we evaluate the performance of the proposed algorithm for Model B, which is the mixed-integer linear model derived from the proposed non-linear one. We consider the scenario described in Section 7 with $CR = 90$ cm for relays since it both increases the complexity of the network topology and is more practical in real situations.
We first compare the following methods with each other.

- **CPLEX**: a state-of-the-art Branch and Cut solver (IBM ILOG CPLEX 11);
- **Algo1**: Our cutting plane algorithm-based heuristic;
- **Algo2**: Our cutting plane algorithm-based heuristic with warm-start strategy.

Model	E_{tot} (μJ/bit)	$E_S(\mu J/bit)$	N_R
Single-hop (Bilandi et al. 2021 [18])	10.347	0.795	-
Multi-hop sensor-base (Reusens et al. 2009 [30])	3.18	0.244	-
Multi-hop relay-base (Bilandi et al. 2021 [18])	1.301	0.064	3
Relay Network (Ehyaie et al. 2009 [15])	0.964	0.017	14
EAWD (p=200,$CR = 30\ cm$) (Elias 2014 [17])	1.066	0.017	7.5
EAWD (p=200,$CR = 90\ cm$) (Elias 2014 [17])	0.686	0.017	3
Model A (U=200,$CR = 30\ cm$)	1.304	0.017	7
Model A (U=200,$CR = 90\ cm$)	0.906	0.017	3

Table 10
Models' comparison in the WBAN scenario: total energy per bit consumed by (1) the whole network and (2) each biosensor, and (3) the number of relays installed in the WBAN (in average), in the approaches introduced in [15, 17, 18, 30], and with our proposed model A

Multi-hop		Relaing network		EAWD		Model B	
routing	Re^{path}	routing	Re^{path}	routing	Re^{path}	routing	Re^{path}
$A \to S$	0.8704	$A \to r_1 \to r_2 \to s$	0.936	$A \to r_{79} \to r_{67} \to r_{58} \to s$	0.2	$A \to r_{80} \to r_{68} \to s$	0.842
$B \to S$	0.4816	$B \to s$	–	$B \to r_{40} \to s$	0.87	$B \to r_{62} \to s$	0.870
$C \to S$	0.8704	$C \to s$	–	$C \to r_{57} \to s$	0.7	$C \to r_{51} \to s$	0.870
$D \to S$	0.19	$D \to r_3 \to s$	0.967	$D \to r_{54} \to r_{57} \to s$	0.68	$D \to r_{55} \to s$	0.870
$E \to A \to S$	0.842	$E \to r_4 \to r_5 \to s$	0.936	$E \to r_{78} \to r_{67} \to r_{58} \to s$	0.16	$E \to r_{70} \to r_{67} \to r_{68} \to s$	0.842
$F \to B \to S$	0.341	$F \to s$	–	$F \to r_{59} \to s$	0.9	$F \to r_{62} \to s$	0.870
$G \to D \to S$	0.165	$G \to r_6 \to s$	0.967	$G \to r_{44} \to r_{41} \to s$	0.8	$G \to r_{34} \to r_{37} \to s$	0.936
$H \to D \to S$	0.165	$H \to r_7 \to s$	0.967	$H \to r_{52} \to r_{57} \to s$	0.6	$H \to r_{52} \to s$	0.842
$I \to F \to B \to S$	0.296	$I \to r_8 \to r_9 \to s$	0.936	$I \to r_{78} \to r_{67} \to r_{58} \to s$	0.16	$I \to r_{78} \to r_{69} \to r_{60} \to s$	0.906
$J \to C \to S$	0.842	$J \to r_{10} \to s$	0.967	$J \to r_{40} \to s$	0.8	$J \to r_{36} \to s$	0.968
$K \to G \to D \to S$	0.160	$K \to r_{11} \to r_{12} \to s$	0.936	$K \to r_{15} \to r_{32} \to r_{41} \to s$	0.8	$K \to r_{24} \to r_{25} \to r_{55} \to s$	0.815
$L \to H \to D \to S$	0.160	$L \to r_{13} \to s$	0.967	$L \to r_{56} \to s$	0.9	$L \to r_{70} \to s$	0.968
$M \to I \to F \to B \to S$	0.287	$M \to r_{14} \to r_{15} \to s$	0.936	$M \to r_{75} \to r_{78} \to r_{67} \to s$	0.3	$M \to r_{72} \to r_{58} \to r_{59} \to s$	0.906

Table 11
WBAN scenario: comparison of the approaches introduced in [15, 17, 18, 30] and with our proposed Model B in terms of reliability for the case U=80, d_b^s=45 kb, and τ^b=0.8

The program's runtime (in seconds) and the relative gap are used to measure performance for comparison purposes. Given the E_{tot}, E_{tot}^L, E_{tot}^U values, the optimality gap (Gap(%)) for the lower bounding model is then calculated as $|100(E_{tot} - E_{tot}^L)/E_{tot}|$, and the same calculation goes for the upper bounding model. If the algorithm fails to find any feasible solution, the reported optimality gap is set to 100%.
Table 13 shows the results for the different methods by varying the number of candidate sites for relays installation (U) from 40 to 200.
As reported in Table 13, solving the problem with CPLEX takes 2 minutes for the $U = 40$ case and up to 9 hours when U is set to 200. On the other hand, **Algo1** can reduce computational time from 1 minute to 7 hours; however, the

Methods	Re^{path}		
	Min	Avg	Max
Multi-hop	0.16	0.369	0.870
Relay network	0.936	0.731	0.967
EAWD	0.16	0.605	0.9
Model B	0.815	0.885	0.968

Table 12
WBAN scenario: comparison of the approaches introduced in [15, 17, 18, 30] and with our proposed Model B based on three indexes: Min, Avg and Max values of path reliability.

U	CPLEX		Algo 1				Algo 2			
			LB		UB		LB		UB	
	Time	E_{tot}	Time	Gap(%)	Time	Gap(%)	Time	Gap(%)	Time	Gap(%)
40	121.104	906.744	61.085	0.19	63.751	0.08	20.637	0.19	21.486	0.08
50	250.958	906.621	104.925	0.1	110.688	0.02	35.133	0.1	37.107	0.02
60	368.706	906.183	164.096	0.04	180.271	0.01	70.758	0.04	70.505	0.01
80	830.618	906.04	319.636	0.22	343.103	0.03	142.679	0.22	167.311	0.03
100	1529.496	936.035	728.074	0.13	828.86	0.13	378.625	0.13	426.028	0.13
150	9894.618	905.929	4531.164	0.203	4989.737	0.214	1431.1	0.203	1824	0.214
200	32464.982	905.77	23532.853	0.3	25297.967	0.279	2314.801	0.3	2453.83	0.279

Table 13
Computation time: comparison of three methods (CPLEX, Algo 1, and Algo 2).

extent of this reduction is not significant for large scenarios. If we apply a warm-start strategy to generate an initial set of tight cuts, the optimal solution to the problem can be found in at least 20 seconds and at most in 2 hours for the lower bound model (approximately 3 hours for the upper bound model). As can be seen in Figure 9, solving the REAWD problem using the warm-start strategy takes only 17% of CPLEX computational time for the $U = 40$ case. Although the trend is a bit fluctuating for different U values, solving the problem with this method needs at most 31% of the time that is taken by the CPLEX method (for the case in which $U = 200$). In other words, using our proposed warm-start strategy on the different scenarios with different U values, reduces the computation time by at least 69%, and at most 90% (for huge scenarios), with respect to the CPLEX method. Then, **Algo1** has, on average, better results than CPLEX, but **Algo2** has the best results and provides better performance rather than the other. Results show that generating an initial set of tight cuts to **Algo2** improves the performance consistently. Hence, we use **Algo2** in our remaining experiments.

Table 14 shows the computational result of the proposed algorithm and Cplex for different scenarios. For this comparison, various scenarios (27 in total) that are representative of real patient monitoring situations are investigated. Each instance that is illustrated in the column named *"scenario"* is defined as a triple subset of three restricted sets $U = \{60, 80, 100\}$, $\tau^b = \{0.4, 0.6, 0.8\}$, and $d^b(kb) = \{40, 65, 90\}$ which contain Min(1), AVE(2), and Max(3) values of ordered sets U, τ^b, and d^b. For instance, the components of scenario "132" consist of Min, Max, and AVE values of sets U, τ^b, and d^b, respectively. Hence, for the "132" scenario, parameters U, τ^b, and d^b are set to $60, 0.8, 90$, respectively. Two notable observations can be made from Table 14. First, the optimality Gap in both presented schemes is less than 1%. To provide more details, the achieved optimality Gap in the lower bounding model is less than 0.7% for almost half of the scenarios, and this value improved to zero for about 41% of them. In the upper bounding scheme, there is no optimality Gap for 29.6 % of the scenarios, and for the rest of them, the optimality gap is less than 0.7%.

Second, our approach reduces the computation time by more than 90% for all investigated scenarios in both schemes

Scenario	Model B		Lower bounding scheme		Upper bounding scheme	
	E_{tot}(nJ/bit)	Time(s)	Time(s)	Gap(%)	Time(s)	Gap(%)
111	36194400	1904.944	82.865	0.58	85.912	0.58
112	58816000	816.645	15.271	0	15.271	0.58
113	81437390	1040.503	19.873	0.11	19.145	0
121	36194400	504.814	27.613	0.58	28.421	0.58
122	58815890	779.435	16.679	0	16.368	0.58
123	81437700	2011.607	29.771	0	26.754	0
131	36194400	432.128	49.781	0	65.683	0.5
132	58816120	2593.981	105.315	0.3	33.462	0.32
133	81437700	2496.898	101.374	0	98.627	0
211	36195270	1669.816	61.783	0.6	63.453	0.6
212	58817320	2049.35	27.461	0.6	29.100	0.6
213	81439370	2827.346	25.446	0.2	31.949	0.07
221	36195270	1245.058	50.798	0.6	52.914	0.6
222	58817320	1716.869	27.298	0.6	30.216	0.6
223	81442930	3839.07	88.298	0	35.319	0.007
231	36195270	1470.914	95.609	0	145.914	0.6
232	58819900	8579.737	54.052	0.08	78.07	0.17
233	81442930	11920.668	232.453	0	239.60	0
311	36192930	3076.151	85.824	0.6	87.977	0.6
312	58813510	11428.739	42.286	0.65	44.572	0.6
313	81434090	5132.854	32.850	0.4	44.655	0.3
321	36192930	2189.917	84.311	0.65	89.129	0.67
322	58813510	3578.387	43.29 8	0.6	46.161	0.6
323	81434170	14019.374	70.096	0	44.861	0.65
331	36192930	2479.005	161.879	0	251.371	0
332	58813570	9268.947	85.274	0.3	139.034	0.16
333	81434170	13534.611	457.469	0	419.572	0

Table 14
Computational results of the proposed algorithm and Cplex for different scenarios.

(just in three instances, this value is more than 84%). To conclude, increasing the values of parameters U, τ^b, and d^b one by one or all of them together, is effect-less in increasing the computation time and optimality Gap.

9. Conclusion

The purpose of this paper is to develop an efficient heuristic algorithm to solve the proposed Reliable and Energy-Aware Wireless Body Area Network Design (REAWD) problem in an acceptable amount of time. In the REAWD problem, we focus on the idea of controlling traffic congestion on intermediate nodes in WBANs, considering both network reliability and network lifetime challenges. To face these issues, we proposed multi-hop relay-based communication and relay placement as two network substructures. To handle the congestion of the incoming traffic to each relay and provide reliable data transmission from each biosensor toward the sink, the product of the reliability

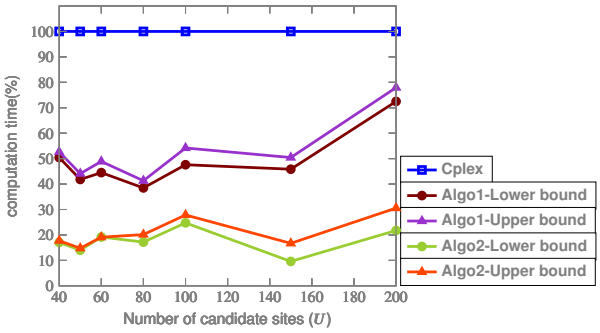

Figure 9: Computation time of linearized REAWD instances using three methods.

functions of relays that are deployed on each biosensor to the sink path must satisfy a given probability threshold value.

We address two common and fundamental issues in WBANs, related to the quality of services: network lifetime and reliability. We first formulate the problem as an NP-hard non-linear mixed-integer program, and numerical results show that state-of-the-art commercial solvers, like CPLEX, cannot solve it in polynomial or reasonable time even for small-size scenarios. To deal with the complexity of this problem, therefore, we first provide a linearized version of the model and then execute a cutting plane algorithm-based heuristic on its associated lower and upper bounding scheme, which provides a significant improvement in terms of computation time, but is still not sufficient, especially for large instances (for example, when $U = 200$). To speed up the computation of the optimal solution in every instance of the problem, we propose a heuristic technique on master problems to reach an efficient initial solution. Numerical results show that our proposed algorithm reduces computation time by about 69% (at least) with respect to the exact model for large scenarios.

We have tested the functionality of the REAWD model by setting different values for its parameters like data rate (d), the number of candidate sites for relays (U), and the probability threshold parameter (τ). Numerical results show that our model can provide a good trade-off between network reliability and energy consumption using the least number of relays which provide efficient monitoring without putting any restrictions on body movement. Besides, the possibility to adjust the threshold probability parameter leads to distributing traffic on relays in a balanced manner, and further has a considerable effect on minimizing the network energy consumption. Our model is very promising in practice and could cover other WBAN (and, in general, IoT) applications since it captures key performance figures typical of any IoT application, i.e., ensuring a reliable data transfer while controlling delay and data loss. As a future work, we can improve the performance of the proposed model by considering QoS and data priority as two important issues while performing data routing/delivery from the biosensors to the sink. There are different techniques that can be adopted to prioritize data and ensure different QoS. i- we may use priority queues at relay nodes to differentiate between high and low traffic/data priority. ii- We may define different priority levels and let our model compute and deliver first the traffic with the highest priority, then the traffic of the second highest priority, etc., down to the lowest priority. Moreover, on-the-fly WBAN design re-optimization will be analyzed to extend the present work taking explicitly into account WBAN mobility to deal with patient's body posture changes.

Acknowledgements

We acknowledge support from the Iran National Science Foundation (INSF) under Grant 4002549.

References

[1] Shashank Kumar, Arjit Kaur Arora, Parth Gupta, and Baljit Singh Saini. *A Review of Applications, Security and Challenges of Internet of Medical Things*, pages 1–23. Springer International Publishing, Cham, 2021.

[2] Sahshanu Razdan and Sachin Sharma. Internet of medical things (IoMT): overview, emerging technologies, and case studies. *IETE Technical Review*, 39(4):775–788, 2022.

[3] Sonam Lata, Shabana Mehfuz, and Shabana Urooj. Secure and reliable wsn for internet of things: Challenges and enabling technologies. *IEEE Access*, 9:161103–161128, 2021.

[4] G. Elhayatmy, Nilanjan Dey, and Amira S. Ashour. Internet of things based wireless body area network in healthcare. In Nilanjan Dey, Aboul Ella Hassanien, Chintan Bhatt, Amira S. Ashour, and Suresh Chandra Satapathy, editors, *Internet of Things and Big Data Analytics Toward Next-Generation Intelligence*, pages 3–20. Springer International Publishing, Cham, 2018.

[5] Rajeev Sharma and Sandeep Singh Kang. WBAN for healthcare applications: A survey of current challenges and research opportunities. *Journal of Critical Reviews*, 7(17):2444–2453, 2020.

[6] M Alper Akkaş, Radosveta Sokullu, and H Ertürk Cetin. Healthcare and patient monitoring using iot. *Internet of Things*, 11:100173, 2020.

[7] Onorato d'Angelis, Lazzaro Di Biase, Luca Vollero, and Mario Merone. Iot architecture for continuous long term monitoring: Parkinson's disease case study. *Internet of Things*, 20:100614, 2022.

[8] Marwa Salayma. *Reliable and energy efficient scheduling protocols for wireless body area networks (WBAN)*. PhD thesis, 2019.

[9] Tushar Bhardwaj and Subhash Chander Sharma. Cloud-wban: an experimental framework for cloud-enabled wireless body area network with efficient virtual resource utilization. *Sustainable Computing: Informatics and Systems*, 20:14–33, 2018.

[10] Antonio Iyda Paganelli, Pedro Elkind Velmovitsky, Pedro Miranda, Adriano Branco, Paulo Alencar, Donald Cowan, Markus Endler, and Plinio Pelegrini Morita. A conceptual iot-based early-warning architecture for remote monitoring of covid-19 patients in wards and at home. *Internet of Things*, 18:100399, 2022.

[11] K. Narendra Swaroop, Kavitha Chandu, Ramesh Gorrepotu, and Subimal Deb. A health monitoring system for vital signs using iot. *Internet of Things*, 5:116–129, 2019.

[12] M Abdul Jawad and Farida Khurshid. A review of approaches to energy aware multi-hop routing for lifetime enhancement in wireless sensor networks. In *Proceedings of the International e-Conference on Intelligent Systems and Signal Processing*, pages 739–757. Springer, 2022.

[13] Farman Ullah, M Zahid Khan, Gulzar Mehmood, Muhammad Shuaib Qureshi, and Muhammad Fayaz. Energy efficiency and reliability considerations in wireless body area networks: A survey. *Computational and Mathematical Methods in Medicine*, 2022:1–15, 2022.

[14] Avani Vyas, Sujata Pal, and Barun Kumar Saha. Relay-based communications in wbans: A comprehensive survey. *ACM Computing Surveys (CSUR)*, 54(1):1–34, 2021.

[15] Aida Ehyaie, Massoud Hashemi, and Pejman Khadivi. Using relay network to increase life time in wireless body area sensor networks. In *IEEE international symposium on a world of wireless, mobile and multimedia networks & workshops*, pages 1–6. IEEE, 2009.

[16] Tushar Kanta Samal, Sushree Chinmayee Patra, and Manas Ranjan Kabat. An adaptive cuckoo search based algorithm for placement of relay nodes in wireless body area networks. *Journal of King Saud University-Computer and Information Sciences*, 2019.

[17] Jocelyne Elias. Optimal design of energy-efficient and cost-effective wireless body area networks. *Ad Hoc Networks*, 13:560–574, 2014.

[18] Naveen Bilandi, Harsh K Verma, and Renu Dhir. hpso-sa: hybrid particle swarm optimization-simulated annealing algorithm for relay node selection in wireless body area networks. *Applied Intelligence*, 51(3):1410–1438, 2021.

[19] Naveen Bilandi, Harsh K Verma, and Renu Dhir. Energy-efficient relay node selection scheme for sustainable wireless body area networks. *Sustainable Computing: Informatics and Systems*, 30:100516, 2021.

[20] Umer F Abbasi, Noman Haider, Azlan Awang, and Komal S Khan. Cross-layer mac/routing protocol for reliable communication in internet of health things. *IEEE Open Journal of the Communications Society*, 2:199–216, 2021.

[21] Omar Ahmed, Fuji Ren, Ammar Hawbani, and Yaser Al-Sharabi. Energy optimized congestion control-based temperature aware routing algorithm for software defined wireless body area networks. *IEEE Access*, 8:41085–41099, 2020.

[22] Mohammed Abdulrahman Dawood Al-Obaidi and Abdullahi Abdu Ibarahim. R-simple: Reliable stable increased-throughput multi-hop protocol for link efficiency in wireless body area networks. In *2020 International Congress on Human-Computer Interaction, Optimization and Robotic Applications (HORA)*, pages 1–5. IEEE, 2020.

[23] Sudip Misra, Pradyumna Kumar Bishoyi, and Subhadeep Sarkar. I-mac: In-body sensor mac in wireless body area networks for healthcare iot. *IEEE Systems Journal*, 15(3):4413–4420, 2020.

[24] Shuvabrata Bandopadhaya, Rajiv Dey, and Ashok Suhag. Integrated healthcare monitoring solutions for soldier using the internet of things with distributed computing. *Sustainable Computing: Informatics and Systems*, 26:100378, 2020.

[25] Deepak Sethi, Partha Pratim Bhattacharya, Rajeev Kumar, Naveen Chauhan, Narottam Chand, Shuyan Xiao, Shuqi Liu, Yang Yu, Gilbert Nwankwo, Sabah Mohammed, et al. A Comparative Analysis of Single-Hop and Multi-hop transmission using EERDT Protocol in Mobile and Critical Scenario for WBAN. *International Journal of Multimedia and Ubiquitous Engineering*, 12(9):1–14, 2017.

[26] Da-Ren Chen and Wei-Min Chiu. Collaborative link-aware protocols for energy-efficient and qos wireless body area networks using integrated sensors. *IEEE Internet of Things Journal*, 5(1):132–149, 2017.

[27] S Ezhil Pradha, A Moshika, N Balaji, K Andal, G Sambasivam, and M Shanmugam. Scheduled access strategy for improving sensor node battery life time and delay analysis of wireless body area network. *IEEE Access*, 2021.

[28] Smita Sharma, MM Tripathi, and VM Mishra. Comparative analysis of routing protocols in wireless body area network (wban). In *2022 2nd International Conference on Innovative Practices in Technology and Management (ICIPTM)*, volume 2, pages 703–706. IEEE, 2022.

[29] Aan Nazmus Sakib, Micheal Drieberg, Sohail Sarang, Azrina Abd Aziz, Nguyen Thi Thu Hang, and Goran M Stojanović. Energy-aware qos mac protocol based on prioritized-data and multi-hop routing for wireless sensor networks. *Sensors*, 22(7):1–25, 2022.

[30] Elisabeth Reusens, Wout Joseph, Benoît Latré, Bart Braem, Günter Vermeeren, Emmeric Tanghe, Luc Martens, Ingrid Moerman, and Chris Blondia. Characterization of on-body communication channel and energy efficient topology design for wireless body area networks. *IEEE Transactions on Information Technology in Biomedicine*, 13(6):933–945, 2009.

[31] Bolaji Omodunbi, Justice O Emuoyibofarhe, Tayo O Arulogun, John Oladosu, Ibrahim Adeyanju, Olatayo Olaniyan, Nnamdi Okomba, and Adebimpe Esan. Energy optimization algorithm for path selection in wireless body sensor networks. *Current Applied Science and Technology*, 22(1):1–15, 2022.

[32] Ameneh Rostampour, Neda Moghim, and Marjan Kaedi. A new energy-efficient topology for wireless body area networks. *Journal of medical signals and sensors*, 7(3):163–169, 2017.

[33] Yang Zhou, Zhengguo Sheng, Chinmaya Mahapatra, Victor CM Leung, and Peyman Servati. Topology design and cross-layer optimization for wireless body sensor networks. *Ad Hoc Networks*, 59:48–62, 2017.

[34] Brian Cornet, Hua Fang, Hieu Ngo, Edward W Boyer, and Honggang Wang. An overview of wireless body area networks for mobile health applications. *IEEE Network*, 36(1):76–82, 2022.

[35] Hashim A Hashim, Babajide Odunitan Ayinde, and Mohamed A Abido. Optimal placement of relay nodes in wireless sensor network using artificial bee colony algorithm. *Journal of Network and Computer Applications*, 64:239–248, 2016.

[36] Chenyang Zhou, Anisha Mazumder, Arun Das, Kaustav Basu, Navid Matin-Moghaddam, Saharnaz Mehrani, and Arunabha Sen. Relay node placement under budget constraint. In *Proceedings of the 19th International Conference on Distributed Computing and Networking*, pages 1–11, 2018.

[37] Milen Nikolov and Zygmunt J Haas. Relay placement in wireless networks: Minimizing communication cost. *IEEE transactions on wireless communications*, 15(5):3587–3602, 2016.

[38] Ragheb Rahmaniani, Teodor Gabriel Crainic, Michel Gendreau, and Walter Rei. Accelerating the benders decomposition method: Application to stochastic network design problems. *SIAM Journal on Optimization*, 28(1):875–903, 2018.

[39] Matteo Fischetti, Domenico Salvagnin, and Arrigo Zanette. A note on the selection of benders' cuts. *Mathematical Programming*, 124(1):175–182, 2010.

[40] Hugues Marchand, Alexander Martin, Robert Weismantel, and Laurence Wolsey. Cutting planes in integer and mixed integer programming. *Discrete Applied Mathematics*, 123(1-3):397–446, 2002.

[41] Dimitris Bertsimas, Ryan Cory-Wright, and Jean Pauphilet. A unified approach to mixed-integer optimization problems with logical constraints. *SIAM Journal on Optimization*, 31(3):2340–2367, 2021.

[42] Amitabh Basu, Michele Conforti, Marco Di Summa, and Hongyi Jiang. Complexity of branch-and-bound and cutting planes in mixed-integer optimization. *Mathematical Programming*, pages 1–24, 2022.

[43] Ramanpreet Kaur, Bikram Pal Kaur, Ruchi Pasricha Singla, and Jaskirat Kaur. Amerp: Adam moment estimation optimized mobility supported energy efficient routing protocol for wireless body area networks. *Sustainable Computing: Informatics and Systems*, 31:100560, 2021.

[44] Jocelyne Elias, Abdallah Jarray, Javier Salazar, Ahmed Karmouch, and Ahmed Mehaoua. A reliable design of wireless body area networks. In *2013 IEEE Global Communications Conference (GLOBECOM)*, pages 2742–2748. IEEE, 2013.

[45] April K Andreas and J Cole Smith. Mathematical programming algorithms for two-path routing problems with reliability considerations. *INFORMS Journal on Computing*, 20(4):553–564, 2008.

[46] Laurence A Wolsey. *Integer programming*. John Wiley & Sons, 2020.

[47] Zeinab Shahbazi and Yung-Cheol Byun. Towards a secure thermal-energy aware routing protocol in wireless body area network based on blockchain technology. *Sensors*, 20(12):1–26, 2020.

[48] Tin-Yu Wu and Cheng-Han Lin. Low-sar path discovery by particle swarm optimization algorithm in wireless body area networks. *IEEE Sensors Journal*, 15(2):928–936, 2014.

[49] Ghufran Ahmed, Saif Ul Islam, Maham Shahid, Adnan Akhunzada, Sohail Jabbar, Muhammad Khurram Khan, Muhammad Riaz, and Kijun Han. Rigorous analysis and evaluation of specific absorption rate (sar) for mobile multimedia healthcare. *IEEE Access*, 6:29602–29610, 2018.

[50] Nordic inc. nrf2401 single chip 2.4 ghz radio transceiver data sheet. http://www.nordicsemi.com/eng/Products/2.4GHz-RF/nRF2401A/(language)/eng-GB.

[51] Vaibhav S Girnale and Harshavardhan B Patil. Review on power amplifier for wsn applications. *International Research Journal of Engineering and Technology (IRJET)*, 4(1):1649–1651, 2017.

[52] Mohammad Dakhel and Sukaina Hassan. Stable high-throughput energy efficiency reliable protocol for wireless body area networks. In *2019 2nd Scientific Conference of Computer Sciences (SCCS)*, pages 32–37. IEEE, 2019.